Review of Palaeobotany and Palynology 280 (2020) 104276

Contents lists available at ScienceDirect

Review of Palaeobotany and Palynology

journal homepage: www.elsevier.com/locate/revpalbo

Birch-sedge communities, forest withdrawal and flooding at the beginning of Heinrich Stadial 3 at the southern Alpine foreland

Cesare Ravazzi [a,*], Federica Badino [a,b], Renata Perego [a], Paolo Bertuletti [c], Mattia De Amicis [c], Massimiliano Deaddis [a], Lorena Garozzo [a], Massimo Domenico Novellino [a], Roberta Pini [a]

[a] CNR – Institute of Environmental Geology and Geoengineering (IGAG), Laboratory of Palynology and Palaeoecology, Piazza della Scienza 1, 20126 Milano, Italy
[b] University of Bologna, Dept. of Cultural Heritage, via degli Ariani 1, 48121 Ravenna, Italy
[c] University of Milano – Bicocca, Dept. of Environmental and Earth Sciences, Piazza della Scienza 1, 20126 Milano, Italy

ARTICLE INFO

Article history:
Received 9 May 2020
Received in revised form 26 June 2020
Accepted 27 June 2020
Available online 7 July 2020

Keywords:
Floodplain paleoecology
Betula pubescens
Bark lenticels
Climate-driven alluvial activity
Heinrich Stadial 3
Radiocarbon chronology

ABSTRACT

The southern Alpine foreland, facing windward to moist southern airmasses, is claimed to have supported forest vegetation throughout the Last Glaciation. Here we present a multiproxy paleoecological record from a compressed peat, uncovered at Casaletto Ceredano, N-Italy, spanning the interval from 33 to 30.5 kyr cal BP. Stratigraphically, it underlies a fluvioglacial belt attributed to the Last Glacial Maximum. The peat records a floodplain swamp community with tree birch and tall sedges, pine woodlands in upland areas, and only limited patches of open vegetation. Plant macrofossils – bark, charcoal, wood and fruits – establish the predominant role of *Betula pubescens* group (downy birch) in the anoxic wetland, thanks to its ability to enhance gas exchange through a distinctive type of bark lenticels. A fire-induced birch-to-pine cycle is repeated twice along the 2500 years-time span covered by the peat layer. The climate reconstructed from modern pollen analogs compares to northern boreal zone, with Tjuly <15 °C, excluding warm-temperate trees.

A major flood sealing the swamp with minerogenic silt is precisely dated to 30,497 $\pm$ 594 yr cal BP (2σ uncertainty). Here, the pollen record shows a substantial forest withdrawal, and development of grasslands and semi-deserts, pointing to co-factorial action of increased climate continentality and of river dynamics. According to teleconnections with the Atlantic and Arctic framework of the stadial–interstadial climate variability, the age and pattern of this event are consistent with the onset of Heinrich Stadial 3, causing a lockdown of moist westerlies and of their Rossby waves in the W-Mediterranean.

1. The southern Alpine foreland during the last full glacial. Ecosystems and climate forcings

In order to decipher the effects of last glaciation climate variability at millennial scale in the Alpine region, it is necessary to analyze natural archives with high stratigraphic resolution and accurate dating. This issue is conveniently afforded in lacustrine records and speleothems from the circumalpine region (Wohlfarth et al., 2008), or even formed within the glaciated area (Spötl and Mangini, 2007; Luetscher et al., 2015). However, spectacularly rapid changes also occurred in the alluvial systems connecting the forelands with major glacier spillouts, as their discharge and mineral load increase often anticipated the culmination of glaciers in piedmont amphitheaters (i.e., 26–22 kyr cal BP in the Italian Alps, Monegato et al., 2017 , Fig. 1b). The whole southern Alpine foreland was sealed by megafan progradation, forming fluvioglacial aprons 15–30 m thick (Fontana et al., 2014; Fig. 1b). Disentangling direct climate forcing from indirect disturbance effects, e.g., perturbation related to alluvial activity over piedmont and floodplain ecosystems, is a major challenge in climate–environment reconstruction at the last glacial culmination. Indeed, the distribution of plant communities over a subalpine alluvial fan bears direct links with magnitude and frequency of surface disturbance, and estimated surface age is an important explanatory variable (Lane et al., 2016). Meanwhile, terrestrial ecosystems are anytime affected by the direct action of climate, thus edaphic and climatic forcings co-occur in the alluvial realm and are difficult to separate. Intensification of Alpine glaciation is recorded yet at the age of the Heinrich Stadial 3 (Spötl et al., 2013), at least 4 kyr before the LGM culmination. Between 32 and 30 kyr cal BP, glacier advance in the major Alpine valleys induced a progradation of alluvial–fluvioglacial fans, an increase in sediment load and enhanced perturbation intensity over the alluvial forest communities. Spread of alluvial fans and coeval forest withdrawal are already recorded at the N-Italian foothills around 38 kyr cal BP (Monegato et al., 2011). During these episodes, eolic

* Corresponding author at: CNR-IGAG, Lab. of Palynology and Palaeoecology, Piazza della Scienza 1, 20126 Milano, Italy.
E-mail addresses: cesare.ravazzi@cnr.it (C. Ravazzi), federica.badino@unibo.it (F. Badino), mattia.deamicis@unimib.it (M. De Amicis), roberta.pini@cnr.it (R. Pini).

https://doi.org/10.1016/j.revpalbo.2020.104276
0034-6667/

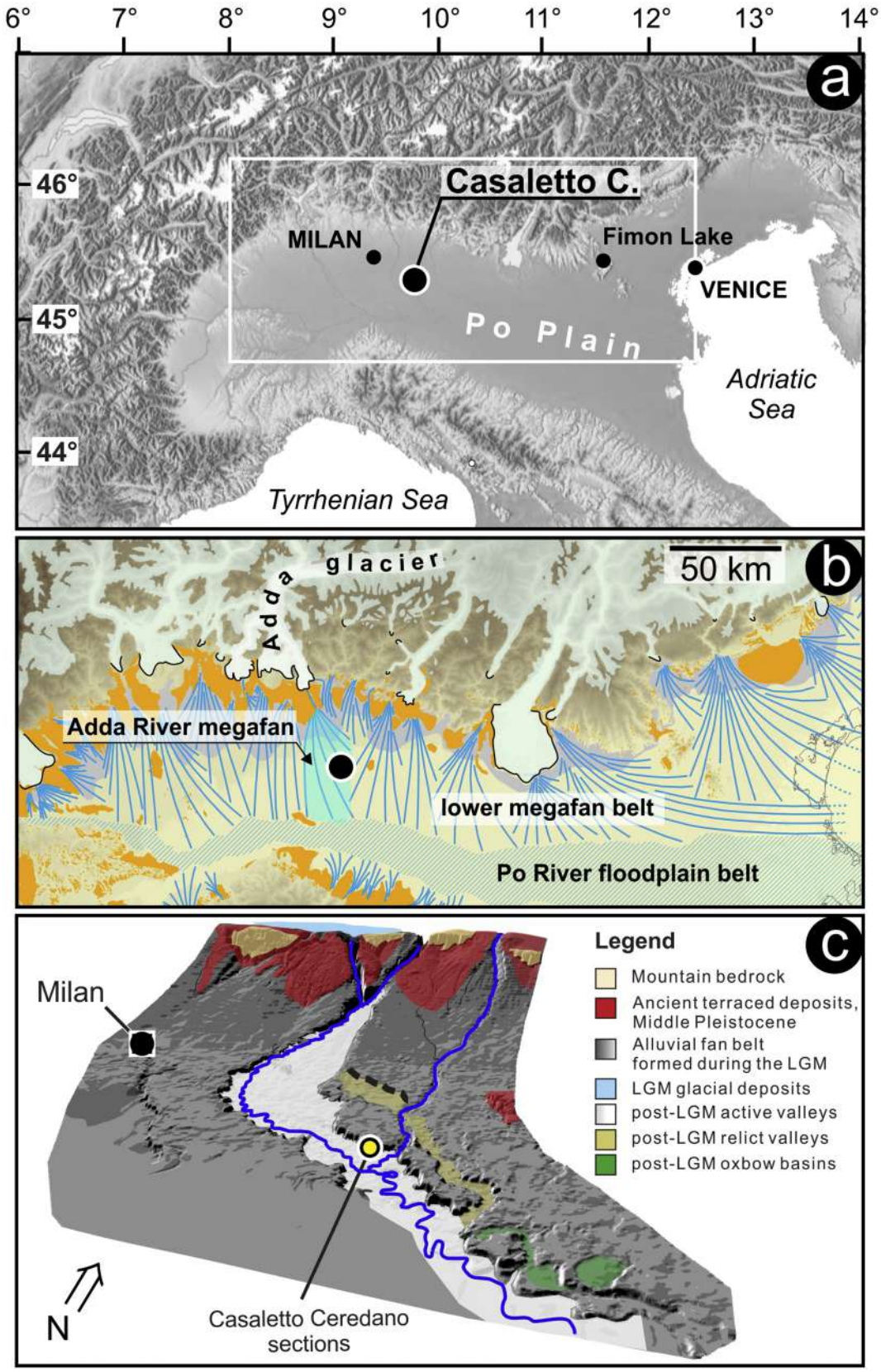

Fig. 1. (1a) Location of the Casaletto Ceredano sections in the southern foreland of the Alps. (1b) Paleogeography of the Italian Forealps and forelands in the early Last Glacial Maximum, 26–22 kyr cal BP, showing glacier extent and front moraines at culmination; stable surfaces with loess (in orange); the megafan belt and the Po River floodplain belt (courtesy group of Paleographic mapping of the Great Adriatic – Padanian Region). Casaletto Ceredano peat is lying 35 km downstream from the LGM front moraines of the eastern lobe of the Adda Glacier, underlying the base deposits of the distal sandur built by the Adda River. (1c) Digital Terrain Model and geological sketch of the study area.

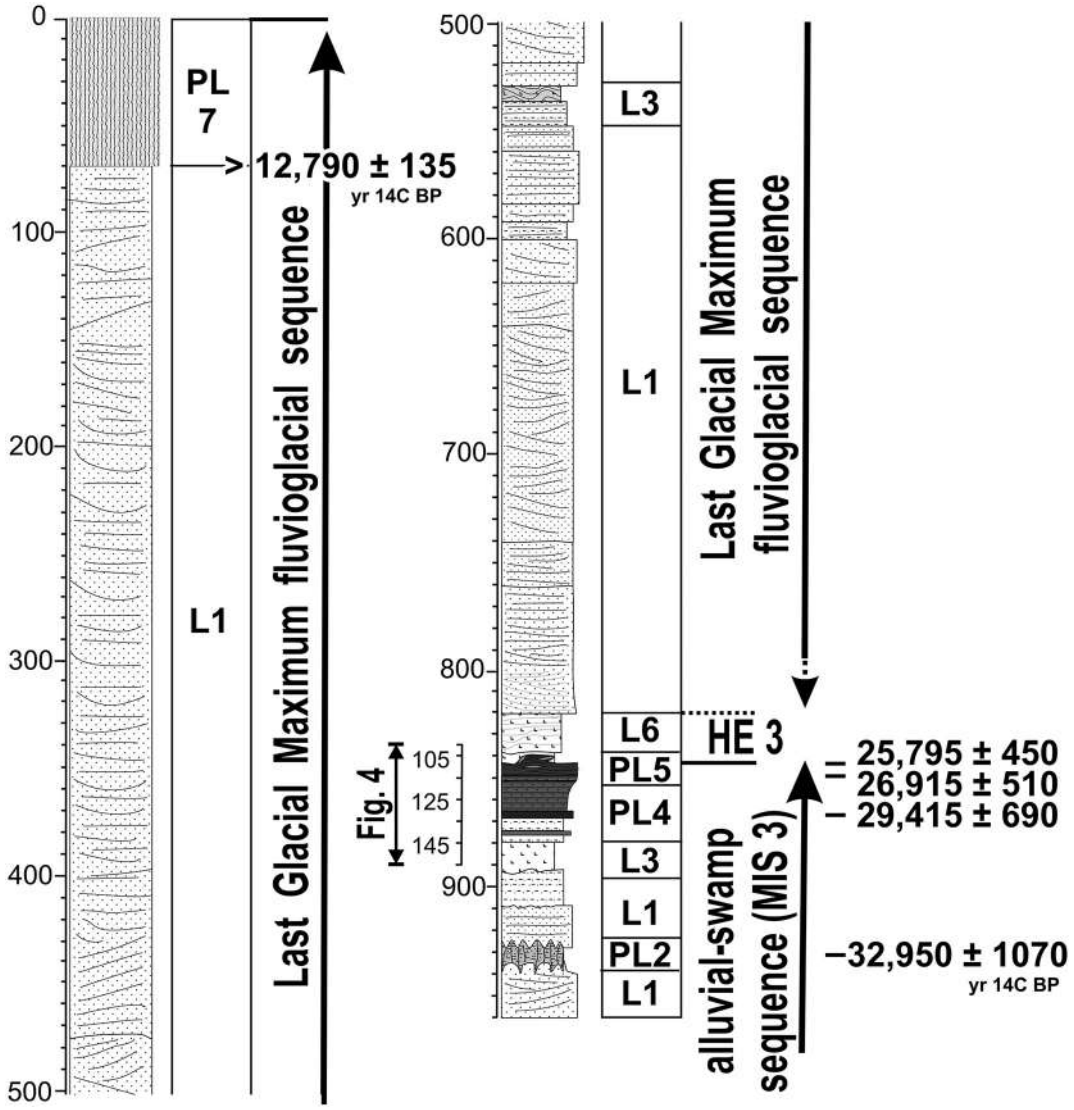

Fig. 2. Summary log of the sedimentary sequence spanning the last 40 kyr in the Central Po Plain as exposed along the eastern scarp of the Adda River valley at Casaletto Ceredano, Coordinates WGS84–45°18′49.75"N 9°37′21.86"E. Compressed peat layer in dark. The complete, composite section was measured from terrace surface downward; however, in the detailed study we will use the measures of the individual peat bog section 1 (see Fig. 3d). Key to acronyms for litho-/pedofacies: L1 – Cross-bedded silty sands; PL2 – Entisol evolved in sands, with pedoturbations, soil surface bearing charcoal fragments; L3 – Gray-blue silty sands (gley); PL4 – Compressed peat admixed to minerogenic silt; PL5 – Compressed peat with wood fragments; L6 – Laminated silt; PL 7 – Alfisol profile (undetailed).

deflation likely occurred along sandy riverbeds, limiting vegetation cover. On the other hand, at the time of maximum aggradation in the LGM, only stable terraced surfaces were partly excluded from active geomorphic processes (Fontana et al., 2014; Fig. 1b). Rapid climate change may be recorded by a direct forcing on vegetation, i.e., an immediate response in the accumulation rate of airborne pollen dispersed by upland trees, and by decennial-scale changes in vegetation of stable upland areas (Badino et al., 2020b). Further effects include plant starvation by low CO_2 levels (Harrison and Prentice, 2003) and disturbance by increased fire frequency, possibly also involving the impact of the Paleolithic man (Kaplan et al., 2016).

Unraveling the local effects of global climate forcings requires a careful analysis of teleconnections. These correlations are reliable in case of well-dated sequences studied at high stratigraphic resolution. Most of Europe experienced forest withdrawal due to cold-continental phases related to the Heinrich Stadials (Sanchez Goñi et al., 2008; Harrison and Sanchez Goñi, 2010). At the onset of Heinrich Stadial 3 boreal forest withdrew from the southern Alpine foothills (Badino et al., in review, see Fig. 1a). In the low latitude Mediterranean region (<45° N), the effect of this dry extreme was subdued, allowing the survival of mesothermophilous trees at low elevation refugia (Tzedakis et al., 2002, 2013). The southern Alpine fringe (45° N), facing windward to moist southern airmasses (Davolio et al., 2016; Rotunno and Houze, 2007), supported boreal woodlands throughout MIS 3 and 2 (Pini et al., 2010; Monegato et al., 2015), but changes in forest cover and fire occurrence paced the interstadial-stadial cyclicity (Badino et al., in review).

Here we focus on floodplain paleoecology connected to glaciated Alps, to unravel the role of edaphic moisture as an additional or alternative water resource for wetland ecosystems in boreal and semiarid climates. Actually, meltwater rivers provided abundant water supply during summertime, which however was only partly available to plants. Water-saturated soils, common in the lower megafan belts, required adaptation to anoxia (Miola et al., 2006), limiting some taiga species (e.g., *Pinus sibirica* Du Tour, *Pinus cembra* L.). Some W-Eurasian birches (*Betula pubescens* Ehrh. and group, *B. nana* L., *B. humilis* Schrank), the gray alder (*Alnus glutinosa* (L.) Gaertner), several willows (*Salix* sspp.) and larches (*Larix decidua* Miller and *L. sibirica* Ledeb.) are well-adapted to wet anoxic pedoclimates, thus forming swamps and bogs

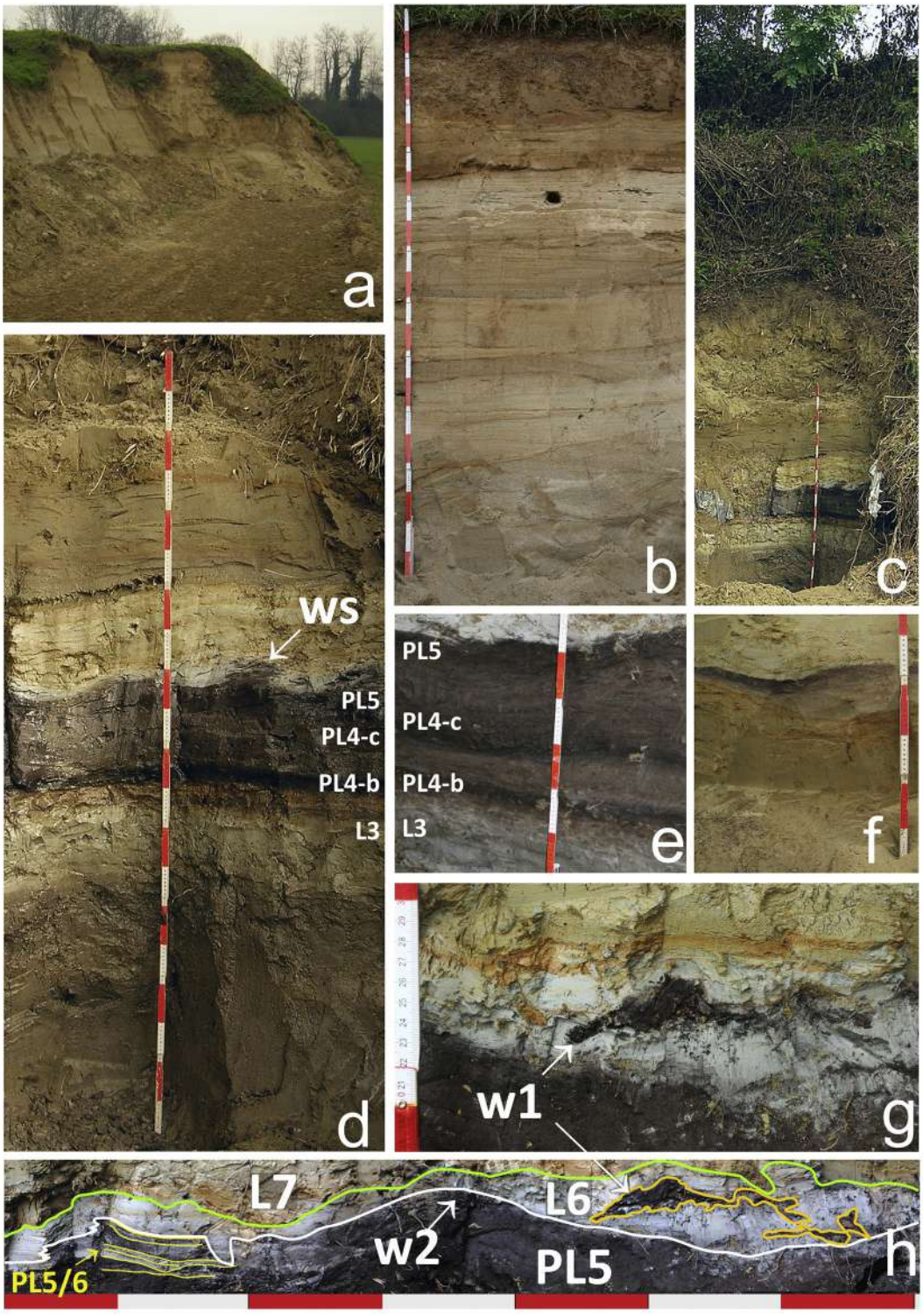

Fig. 3. The succession of alluvial and peat deposits at Casaletto Ceredano, Central Po Plain. (a) The scarp of the terraced alluvial plain exposing the upper part of the depositional sequence, i.e., the fluvioglacial sands. (b) The topmost fluvioglacial sequence and the alfisol evolved at the terraced plain surface. (c, d) The peat layer outcropping at the base of the scarp terrace, and its embedding alluvial deposits, photographed in section 1, sampled for microbotanical stratigraphy. Lithofacies from L3 (gley silt) to PL5 (peat), see Fig. 4. (e) The peat layer, section 2, used as an additional sampling section for macrofossils. Lithofacies from L3 (gley silt) to PL5 (peat), see Fig. 4. (f) Lenticular lateral closure of the peat layer at the border of the wetland basin about 300 m east from the studied sections. (g) Detail of the upper peat/whitish silt contact, showing compressed wood remains (w1) belonging to a birch tree rooted at the top of the peat and resting into silt. Outer rings were dated to 26,312 ± 396 yrs. ^{14}C BP (lab code UBA-42143, see Table 1). (h) Panoramic view of the upper peat PL5/whitish silt L6 contact and the overlying laminated brown silts L7. PL5/6 refers to sets of alternate peat (PL5) and silt laminae (L6) which represent transitional deposition (see Fig. 4 for stratigraphic position) in birch-sedge swamp hollows. Also shown is the position of dated in situ wood samples w1 and w2 and of an in situ birch stump on a small sedge peat mound (ws). Scale - red bars represent 10 cm.

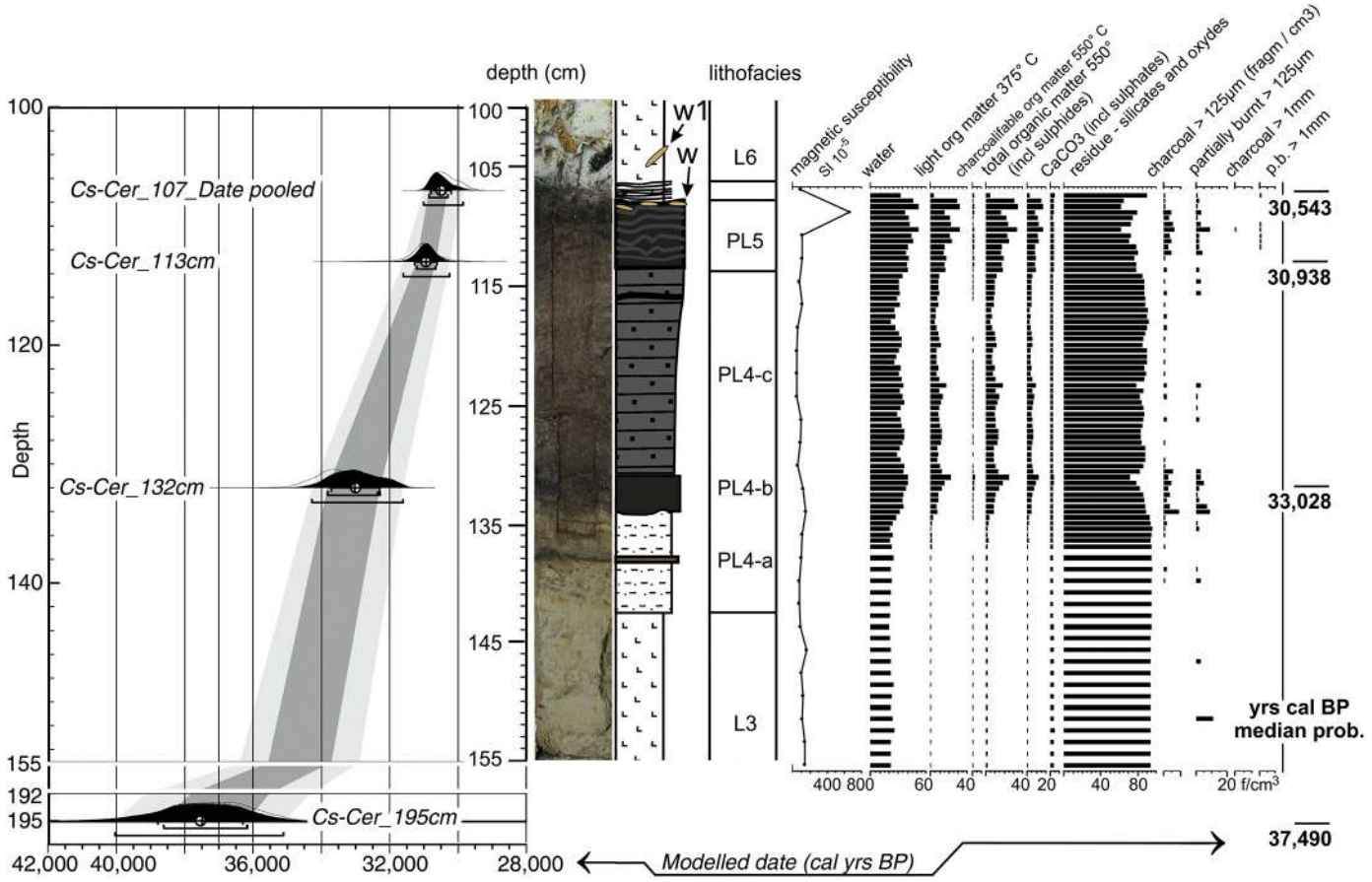

Fig. 4. Chronological model and high-resolution stratigraphy of the peat layer embedded by fine clastic alluvial deposits including loss on Ignition, magnetic susceptibility and sieved charcoal record. Key to the acronyms for lithofacies and pedologic features – see caption Fig. 2.

in boreal wetlands (e.g., Eurola et al., 1984; Walter and Breckle, 1986), while other floodplain trees require periodic watertable oscillations (*Alnus incana* (L.) Moench, *Populus, Hippophäe* and *Picea*).

The alluvial sequence from the last glaciation megafans in the southern Alpine foreland (Fig. 1b) includes several compressed peat layers representing wetland areas and covering wide sectors of the plain (Ravazzi et al., 2012; Hippe et al., 2018). The paleoecological record of one of these wetlands, i.e., the fossil record of a woody mire, is presented here (location in Fig. 1). The peat succession is well-dated and spans the crucial interval of the onset of megafan aggradation at the MIS 3/LGM transition. We provide a high-resolution microbotanical record, supplemented by a comparative study of in situ macrofossils. These consist of remains of bark, wood, charcoals and fruits allowing identification at species level, and inferences on specific ecoclimatic requirements. We used macrofossils to distinguish plants related to the local (anoxic) pedoclimate from upland trees and herbs. Finally, by comparing wetland and upland vegetation changes, and teleconnection with the N-Atlantic climate events, we reconstructed and disentangled direct climate forcing induced by the Heinrich Stadial 3 on pollen production and vegetation from edaphic-driven changes in a fluvioglacial floodplain of southern Europe.

2. Materials and methods

2.1. The studied depositional sequence in the Adda megafan

We studied a 9.60 m-thick sediment sequence outcropping at Casaletto Ceredano, WGS84 45°18′49.75"N 9°37′21.86″E (65 m asl, Fig. 1c) along the eastern scarp of the entrenched Adda River valley. The sequence documents the depositional and environmental history between >40 and 12 kyr cal BP (Fig. 2). The studied site is located in the distal fluvioglacial belt of the Adda River megafan in N-Italy, built between 30 and somewhere before 15 kyr cal BP (Ravazzi et al., 2012; Fig. 1b). Glacier collapse at the end of the Last Glacial Maximum (LGM), around 18–17.5 kyr cal BP (Fontana et al., 2014), prompted fan dissection and the development of the Adda post-glacial valley (Fig. 1c).

The base of the sequence is composed by alluvial sand deposits (lithofacies L1 in Fig. 2), but including an entisol pedoturbated by herb roots (PL2 in Fig. 2). A peat layer at 880–855 cm depth is buried under a thin silty unit (L6 in Fig. 2) in turn covered by a sequence of 820 cm-thick coarse, cross-bedded sands (L1–L3–L1 in Fig. 2). Those sands are considered to represent fluvioglacial aggradation by the braided system belonging to the eastern spill-out of the Adda River (Fig. 1b); their age is constrained between 30 and 15 kyr cal BP (Ravazzi et al., 2012; Fontana et al., 2014), but they formed most probably during the last culmination of Alpine glaciers nowadays dated from 27 to 18 kyr cal BP in the Alps (Monegato et al., 2007) broadly corresponding to the global Last Glacial Maximum (LGM) (Lambeck et al., 2014). On top, an alfisol (PL7, Fig. 3b) evolved during the last 15 kyr cal BP, while the maximum aggradation surface was terraced by the entrenching Adda River floor, downcutting its postglacial valley. The present study focuses on the compressed peat and silty peat recorded between 880 and 855 cm (Figs. 3 and 4) and exposed on the left scarp of the postglacial valley at Casaletto Ceredano (Fig. 3a). It lies at the very base of LGM fluvioglacial sands, thus it may have accumulated at the beginning, or just before, of the LGM glacier culmination in the Alps.

Section 1 was sampled (Fig. 3d) through two 50 cm-long metal boxes. Section 2 (Fig. 3e) was used as an additional sampling section

Table 1
Radiocarbon chronology of the studied section.

Sample position (section, depth)	Dated material	Taphonomy	Laboratory code	^{14}C yr BP	Calibrated 2σ range (cal yr BP)	Calibrated age median probability (cal yr BP)	Pooled mean (^{14}C yr BP)	Modeled median probability (cal yr BP)
Cs-Cer1 107 cm	Outer rings of a tree stem – sample w1 in Fig. 3	In situ	UBA-42143	26,312 ± 396	29,596–31,108	30,483	26,164 ± 297	See below
Cs-Cer1 107 cm	Outer rings of a tree stem – sample w2 in Fig. 3	In situ	Ua-33,261	25,975 ± 450	29,172–30,987	30,144		
Cs-Cer pooled mean 107 cm	Two wood fragments at 107 cm (see above), pooled age	In situ	Pooled mean	26,164 ± 297	29,675–30,964	30,405		30,543
Cs-Cer1 113 cm	Outer rings of a tree stem	In situ	Ua-34,537	26,915 ± 510	29,855–32,034	31,003		30,938
Cs-Cer1 132 cm	cm-sized wood charcoal	Local fire	Ua-34,536	29,415 ± 690	31,781–34,827	33,496		33,028
Cs-Cer1 195 cm	cm-sized wood charcoal	Possibly drifted	Ua-33,262	32,950 ± 1070	34,950–39,922	37,302		37,490

for macrofossils. Sedimentary markers allowed a fine correlation of Sections 1 and 2 (see Fig. 3d and e). For the position of the peat layer in the stratigraphic pattern of the regional fluvial systems, the reader is referred to Ravazzi et al. (2012).

2.2. Palynology, charcoal particles and sediment physical properties

Palynology (37 samples), macroscopic charcoal (56) and Loss on Ignition (81) were studied. Pollen and other microbiological particles were extracted by chemical treatments (acids and KOH), microfiltrations and acetolysis, and identified at the optical microscope, reaching a minimum pollen sum of 500 pollen grains. Cyperaceae pollen, reflecting local changes, was excluded from the pollen sum. Pollen identification followed Beug (2004), Punt and Blackmore (1976-2009), Reille (1992-1998) and the CNR-IGAG pollen reference collection.

Pollen-slide microcharcoal particles were counted under a light microscope at 400x. Black, completely opaque and angular fragments (Clark, 1988) were identified as charcoal and grouped in two size classes (10–50 μm and 50–250 μm length). Furthermore, we recognized sieved charcoal particles from 48 samples processed following Whitlock and Larsen (2001); each sample was soaked for 24 h in a mixture of bleach and sodium hexametaphosphate, then wet-sieved through metal-screened filters with mesh sizes of 125 μm and 1 mm. Each size class was counted under a stereoscope into a gridded Petri dish (Enache and Cumming, 2007; Jensen et al., 2007; Whitlock and Larsen, 2001). Charcoal counts were expressed as particles/cm^3. Diagrams were drawn using Tilia ver.2.0.41 (Grimm, 2015) and Corel Draw X7 for further graphic elaborations.

2.3. Clustering and ordination

Pollen zonation was obtained by constrained incremental sum-of-squares cluster analysis (CONISS, Grimm, 2015). Edwards and Cavalli-Sforza's chord distance was used as dissimilarity coefficient. The analysis runs on taxa displaying statistical significance in proportion values, i.e., those having >2%. Limits of pollen zones coincide with sedimentary changes and thus they were used to subdivide the record into ecostratigraphic phases (acronym CAS, labeled 1–8).

Ordination techniques were applied on the taxa selected for pollen zonation to detect major compositional changes. Given the short gradient length (<2 standard deviation units), principal component analysis (PCA) was preferred to correspondence analysis and performed on the covariance matrix of log-transformed % data (Ter Braak and Prentice, 1988). Data standardization and ordination were carried out with the Vegan and Decorana packages (Oksanen et al., 2019) in R environment (R Core Team, 2013).

2.4. Macrofossil record

The analysis of macroscopic plant remains was carried out on seven sediment samples (Sections 1 and 2; average volume of 308.6 ml) and on selected wood, stump and bark fragments picked up from the stratigraphic Section 2 (see Supplementary Table 1 for details of analyzed samples). The sediment samples were wet sieved at 2–1–0.5–0.125 mm mesh sizes using the wash-over method (Hosch and Zibulski, 2003) and then sorted using a Leica/Wild M3C stereomicroscope with a 6.4–40x magnification.

Identifications of fruits and seeds were made using the CNR-IGAG carpological reference collection, in addition to the specific literature (Bialobrzeska and Trnchanowiczrwna, 1960; Kats et al., 1965; Nilsson and Hjelmquist, 1967; Berggren, 1969; Cappers et al., 2006; Birks, 2007; Bojňanský and Fargašová, 2007; Martinetto et al., 2014). Birch remains (fruits and catkin scales) were identified exclusively on the basis of morphological criteria as a regional dataset of biometric parameters is not available.

The wood and wood charcoal fragments were observed under an episcopic microscope (Zeiss Axio Scope A.1) equipped with dark field/bright field illumination system. Their identification is based on comparison with wood atlases (e.g. Jacquiot et al., 1973; Schweingruber, 1990) and the CNR-IGAG modern anthracological reference collection.

Bark surfaces were cleaned and photographed immediately after recovery. The occurrence and distribution of macroscopic structures (i.e., bark lenticels) were analyzed on bark fragments on a minimum surface of 5 × 5 cm. To examine the taxonomical and ecological value of lenticels in European tree *Betula*, we considered modern populations of *B. pubescens* group and of *B. pendula* both in N-Italy and in Scandinavia.

2.5. Modern taxonomical reference

Nomenclature of modern Eurasian plant *taxa* follows Tutin et al. (1968, 1980, 1993), except for *Betula pubescens* Ehrh. (downy birch). According to the *Flora Europaea* taxonomic system, *B. pubescens* is regarded as a species including a group of several subspecies. However, due to the lack of taxonomical and genomic studies on relict and highly fragmented populations of tree *Betula* today living in the Alps, in the present paper we challenge the species concept for *Betula pubescens* Ehrh. and refer to the group of infraspecific taxa related to it as *B. pubescens* group. North American *taxa* treatment follows Farrar (1995).

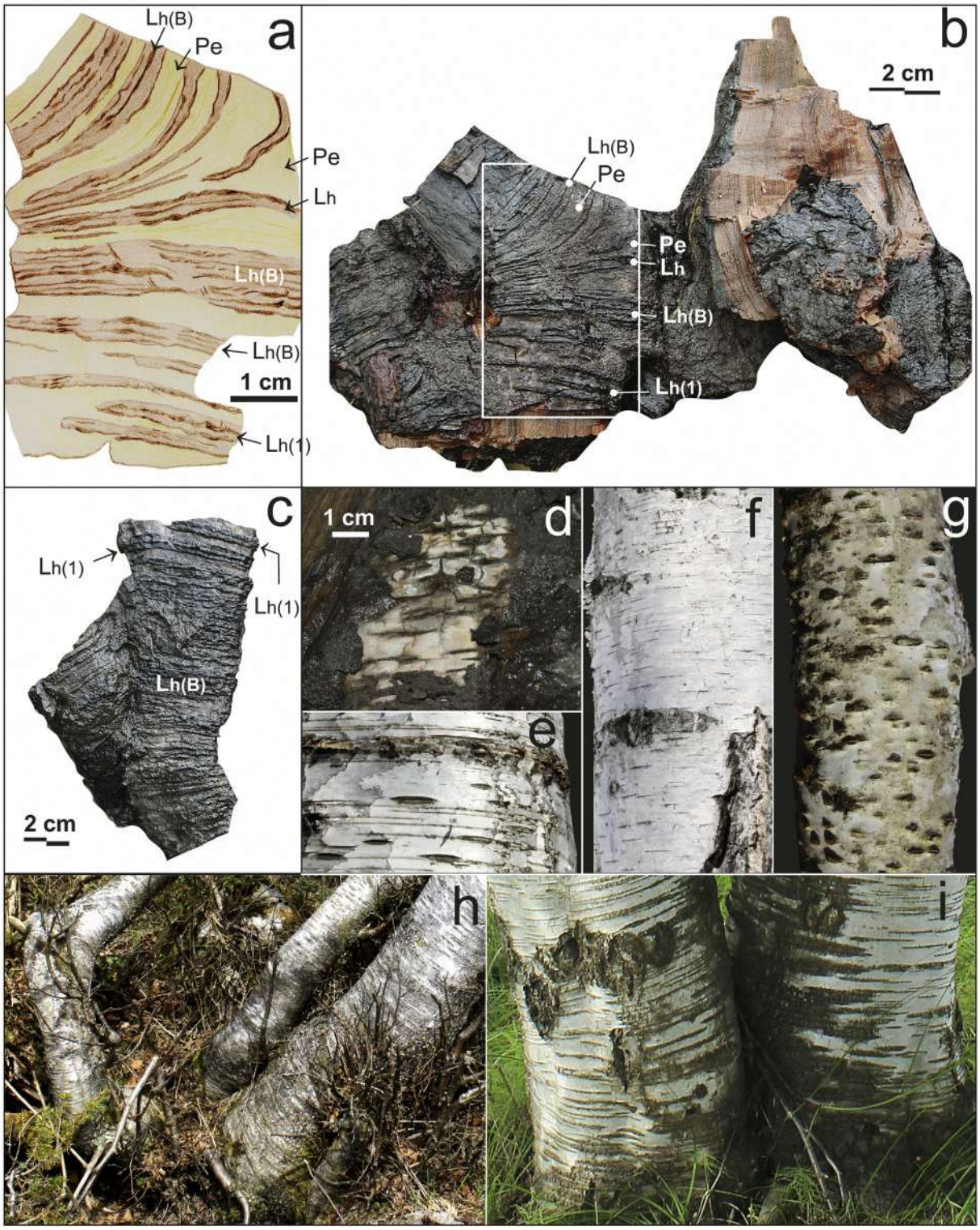

Fig. 5. *Betula pubescens* and *B. alba* cork and variation in lenticel development in the fossil studied material (a–d) and comparative living individuals (e–i). (a) – Outline of the lenticel ridged relief and arrangement in part of the stump (b), drawn at higher magnification; individual streak lenticels – i.e., the type named Lh (1) - are always distinctly ridged and furrowed. (b) – Casaletto Ceredano fossil specimen CAS CER14-8224 - birch stump (*B. pubescens* group) with two stems, showing extensive development of ridged horizontal lenticels, either as individual streaks – Lh(1) type – or associated in multiple bands – Lh(B) type. Smooth, silvery periderm tissue (Pe) is still visible between clusters of lenticel strips. (c) - Casaletto Ceredano fossil specimen CAS CER14-8228 – birch stump showing extensive development of clustered lenticels – Lh(B) type; a few individual lenticels – Lh(1) type – are clearly visible on the uppermost stem segment. (d) – Casaletto Ceredano fossil specimen CAS CER14-8212 – Fragment of rhytidome with silvery preserved periderm surface showing elliptic lenticels – Le type. (e) – Smooth bark in a 30 cm diameter-stem living individual of *B. pendula* growing in *Castanea* woodlands, Italian Forealps (modern specimen MdN-5632) showing both elliptic lenticels – Le type – and linear thin lenticels – Ll type – the latter also clustered in a band. (f) – Smooth and deeply furrowed bark in a 20 cm diameter-stem individual of living *B. pendula* colonizing abandoned meadows, Italian Forealps; lenticels are only of the linear thin Ll type (modern specimen MC-791). (g) – Smooth bark in a 10 cm diameter-stem individual of living *B. pendula* growing into *Castanea* woodlands, Italian Forealps (modern specimen MdN-5626) showing elliptic lenticels – Le type – only. (h) and (i) – Example of development of linear lenticels ring strips in basal stems of *B. pubescens* growing in wet habitats: (h) – from a bog, Schilpario, Italian Forealps (modern specimen Sch-2374). (i) – from a sedge swamp fringing Ounasjoki River, Rovaniemi, Finland (modern specimen Rov-2726, see also Fig. 8b).

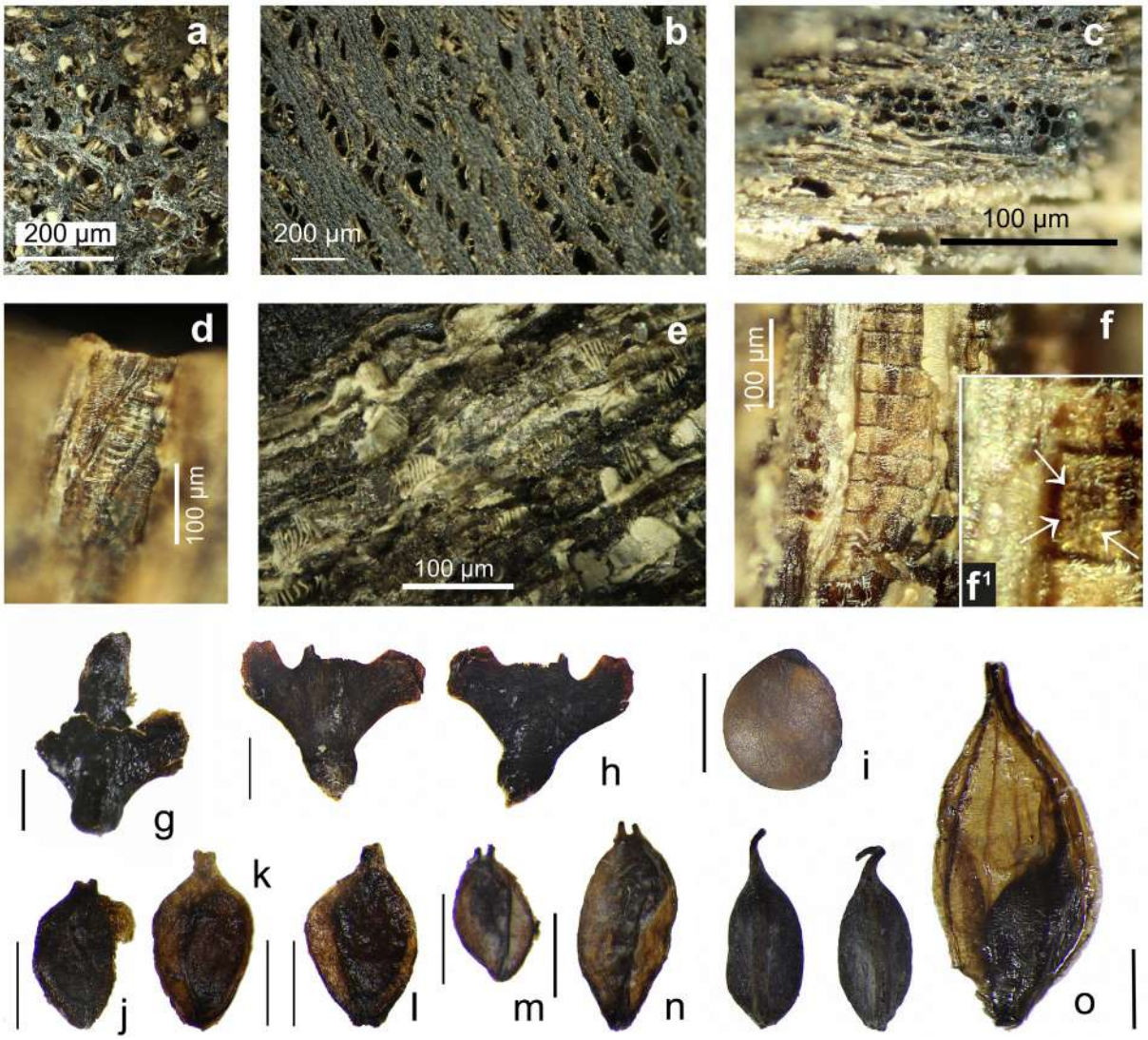

Fig. 6. Selected wood, seeds and fruits from the Casaletto Ceredano peat layer. (a–b) cf. *Betula*, transversal section; section 2 lithofacies PL5 (Fig. 3e); (c) cf. *Betula*, triseriate ray in longitudinal tangential section, section 2, lithofacies PL5; (d) cf. *Betula*, detail of a scalariform perforation plate, section 2, lithofacies PL5; (e) cf. *Betula*, radial longitudinal section, overview of several vessels and scalariform plates remarked by high light reflection, section 2, lithofacies PL5; (f) cf. *Betula*, ray-vessel cross field, section 2, lithofacies PL5; small and numerous pitting can be seen in the close-up (f^1); (g–o) fruits and seeds from the very top of lithofacies PL5 in section 1, see Fig. 3h; (g) *Betula pubescens* group, female catkin scale; (h) *Betula pubescens* group, female catkin scale, abaxial (left) and adaxial (right) views; (i) *Comarum palustre*; (j–m) *Betula* cf. *pubescens* group, fruits; (n) *Betula* cf. *pendula*, fruit; (o) *Carex rostrata/vesicaria*, two achenes and utricule with inner achene and complete style. All wood specimens observed and photographed at the episcopic microscope. Scale bar = 1 mm, unless otherwise specified.

The studied material is stored at the Repository of the Laboratory of Palynology and Palaeoecology, CNR-IGAG located at the Research Area 3 at Milano Bicocca (IT). Codified sample labels are in Suppl. Table 1.

2.6. AMS radiocarbon dating of wood and charcoal

The AMS ^{14}C chronology of the last glaciation >20 kyr cal BP in the Alps is still hampered by the common practice to measure bulk sediment or unidentified organic debris, whose ^{14}C activity may easy be biased by dead carbon and reservoir effects, or natural contamination, especially in lake sediments (e.g., Carcaillet and Blarquez, 2017, Finsinger et al. 2017).

The discovery of datable wood and cm-sized charcoal fragments in several levels of the studied section is of major relevance for the chronology of the last glaciation allowing for precise AMS dating on a high amount (>1 g) of undecayed lignine from compressed wood, or from wood charcoal centimetric fragments. Organic matter reworking is a source of age bias in drift peat imbedded in alluvial and glacial deposits, so we preferred in situ materials (see Table 1). Three samples of wood, including two samples extracted from the external ring set of in situ birch stems, and two charcoal fragments were radiocarbon-dated at the Angstrom Lab., Uppsala University and at the 14C CHRONO Center at Queen's University of Belfast (Table 1). Calibration was carried out using CALIB version 7.0.4 with the IntCal13 atmospheric calibration curve (Reimer et al., 2013). An age-depth model was built up with the Bayesian technique in the Oxcal package v4.3.2 (Bronk Ramsey, 2017), adopting a low flexibility P_Sequence (K = 0.1).

3. Results

3.1. Chronology

The dated wood and charcoal fragments yielded ages spanning a coherent sequence (Table 1 and Fig. 4) between 25,975 ± 450 and 32,950 ± 1070 ^{14}C yr BP. The effects of both contamination and taphonomic reworking were minimized by selecting in situ undecayed wood

or large wood charcoal fragments. The availability of datable wood tissue from tree stems obviously depends on tree occurrence in contemporary vegetation, a circumstance which favorably compares with the forest persistence at several spots in N-Italy throughout the last glaciation (on tree dating in the Alpine LGM see Monegato et al., 2007, 2015).

In order to obtain a precise age from the contact between the topmost peat layer and overlying silt, the ages from the outer rings of two birch stems were pooled; the pooled mean (26,164 ± 297 ^{14}C yr BP) was calibrated (Table 1) and used in the age-depth model. For this level we obtained calibrated ages of 30,405–730/+559 yr cal BP (pooled age median probability and 2σ uncertainty) and of 30,497 ± 594 yr cal BP (modeled pooled age probability and 2σ uncertainty, median 30,543). The posterior analysis of the Bayesian age-depth model supports the reliability of the obtained age sequence between top and base of the compressed peat layer, spanning about 2500 years between 33,028–1715/+1331 and 30,497 ± 594 yr cal BP (2σ uncertainty).

3.2. Identification of downy birch bark remains based on lenticels structure and ecological inferences

Betula, *Alnus* and *Populus* species have phellems with distinctive fossil features such as stratification of thin paper-like layers, and protruding lenticels (Evert, 2006; Pereira, 2017; Shibui and Sano, 2018).

The lenticels borne on smooth bark of native European alders (*Alnus glutinosa* (L.) Gaertner, *A. incana* (L.) Moench., *A. viridis* (L.) Moench.) belong to several structural types, including diamond and horizontal lenticels, combined into distinctive patterns, plus water lenticels at the stem base (McVean, 1956; Shaw et al., 2014). This pattern is not shared by all the American species, some of them bearing the horizontal type only (e.g., *A. incana* subsp. *rugosa* see Farrar, 1995; Nelson et al., 2014).

The whitish or yellowish, young bark of some *Populus* species is characterized by conspicuous diamond lenticels, combined with linear lenticels to develop streaks (Caudullo and de Rigo, 2016a, 2016b).

Typical and distinctive of birch bark are horizontal lenticels (Butler, 1909; Nelson et al., 2014; Shaw et al., 2014). Specifically, in the two main tree birch of Europe (*B. pendula* Roth., silver birch and *B. pubescens* group, downy birch) the horizontal lenticels developing on young, whitish bark may be narrowly elliptic, more or less protruding (Fig. 5e, g) or instead linear-elongated (Fig. 5e–f), while diamond lenticels are inconspicuous (Hynynen et al., 2010; Schweingruber et al., 2019, and personal observations).

The morphological traits of birch bark and of lenticels depend on both taxonomy and ecological environments (Gardiner, 1958 reported in Atkinson, 1992 and personal observations), producing a unique combination of features for given taxa growing in given habitats. This provides the opportunity to investigate the taxonomy and ecology of in situ fossil stumps and stems, as in the case of the present work. The bark of silver birch is fissured by deep and coarse vertical furrows at the old trunk base, disrupting the rhytidome continuity (Hynynen et al., 2010; Schweingruber et al., 2019; Fig. 5f), whereas the downy birch retains smooth bark for many years, exfoliating by thin and small flakes (Hynynen et al., 2010; Fig. 5h, i). Importantly, this type of rhytidome shedding does not disrupt the continuity of horizontal lenticels (personal observations in Alpine populations of *B. pubescens* group), which develop for many years into protruding ring lenticels (Fig. 5h, i) frequently joined into bands (Fig. 5i). Lenticel banding is also related to mechanical stress produced by stem twisting (e.g., Kozlowski, 2012). Indeed, we have observed remarkable ring banding on twisted stems of *B. pubescens* group, while it occurs only at branch bifurcations in *B. pendula*. Functionally, smooth bark enhances corticular photosynthesis (Teskey et al., 2008; Crawford, 2014), while enhanced lenticels area promotes stem aeration in peat bogs and fen environments. Fens are being invaded by downy birch stands in the mixed boreal forest ecosystem especially under high water table (Eurola et al., 1984; see Section 5), thus in poorly aerated soils.

The development of banded and ringed lenticels, strongly protruding over the preserved periderm, has been observed in both stumps which were recovered from the uppermost studied peat sequence (Fig. 5a–c). Diamond lenticels have not been observed. We argue that *B. pubescens*, the downy birch, was growing in situ in the anoxic peat mire during the last phases of peat development, corresponding to pollen zones CAS-5 and CAS-6 in Fig. 7. A few fragments of young bark were also recovered from the same peat levels (Fig. 5d). Although they show the elliptic shape of young linear lenticels protruding over the silvery periderm surface, typical for birch bark, a specific identification was not possible on this material.

3.3. Fruits and woods

Identifiable plant macroremains were mostly retrieved in one sediment sample (see Supplementary Material for details). Despite the total amount of more than 350 remains, only few taxa are represented. Most of these remains are nutlets of *Carex rostrata/vesicaria* some of which still embedded in their utricle (Fig. 6n–o). The morphological characters and sizes of the achenes and the utricles did not match with certainty one of the two *Carex* species. Therefore, we adopted the intermediate taxonomical category for these remains to solve the strong convergence of the two species, at least for what concerns the fruit morphology.

Betula catkin scales offer much more diagnostic features to distinguish species of birches than fossil fruits very often lacking their wings. A few catkin scales have been found in the Casaletto Ceredano peat, whose preservation state (Fig. 6g-h; Suppl. Table 3) prevented any biometrical analysis (Bialobrzeska and Trnchanowiczrwna, 1960; Berglund and Digerfeldt, 1970). Taking into account the high shape variability of catkin scales, either taxonomic or ontogenetic, i.e., the position of scales along the catkin axe, the better-preserved scales were attributed to *B. pubescens* group. The main observed characters are scales longer than broad, with lateral lobes wider and shorter than the central one, in addition to sideways less curved than in *B. pendula*.

In contrast to the catkin scales, fruits of *Betula* are easily identifiable only when they are well-preserved and complete with their wings. Tackling specific determination of wingless *Betula* fruits implied statistical analysis of measured fruitbody parameters (van Dinter and Birks, 1996; Freund et al., 2001). We based our identification only on fruit body morphology due to the relatively low number of measurable items, and the lack of a dataset of *Betula* biometric parameters in the Alpine region. Based on this, all the nutlets found are attributable to tree birches (Fig. 6j–n; Suppl. Table 3). The shrubby species (*B. nana* and *B. humilis*) cannot be taken into account because their nutlets are smaller and comparatively oval and broad. More than 20 nutlets resemble to the *B. pubescens* group while only 2 more likely belong to *B. pendula* (cf). We abstained from further determination within the *B. pubescens* group.

The bad preservation of wood remains, strongly compressed, made their identification rather difficult. Nevertheless, the diagnostic features of the genus *Betula* have been recognized (Fig. 6a–f, Suppl. Table 3). According to the key characters presented by Schweingruber (1990), the occurrence of multiseriate rays as well as the large size of tracheid pores would speak for a birch-tree *taxon* (*B. pubescens* group or *B. pendula*), while excluding shrubby birches (*B. nana* and *B. humilis*), the latter ones bearing uni- to biseriate rays only, aggregate rays occurrence, and smaller size of tracheid pores. The same diagnostic frame would exclude European alders (*Alnus* sspp.). Still, individual specimens may not conform to this taxonomical array, thus we'll cautiously report our wood identifications with the “cf” notation.

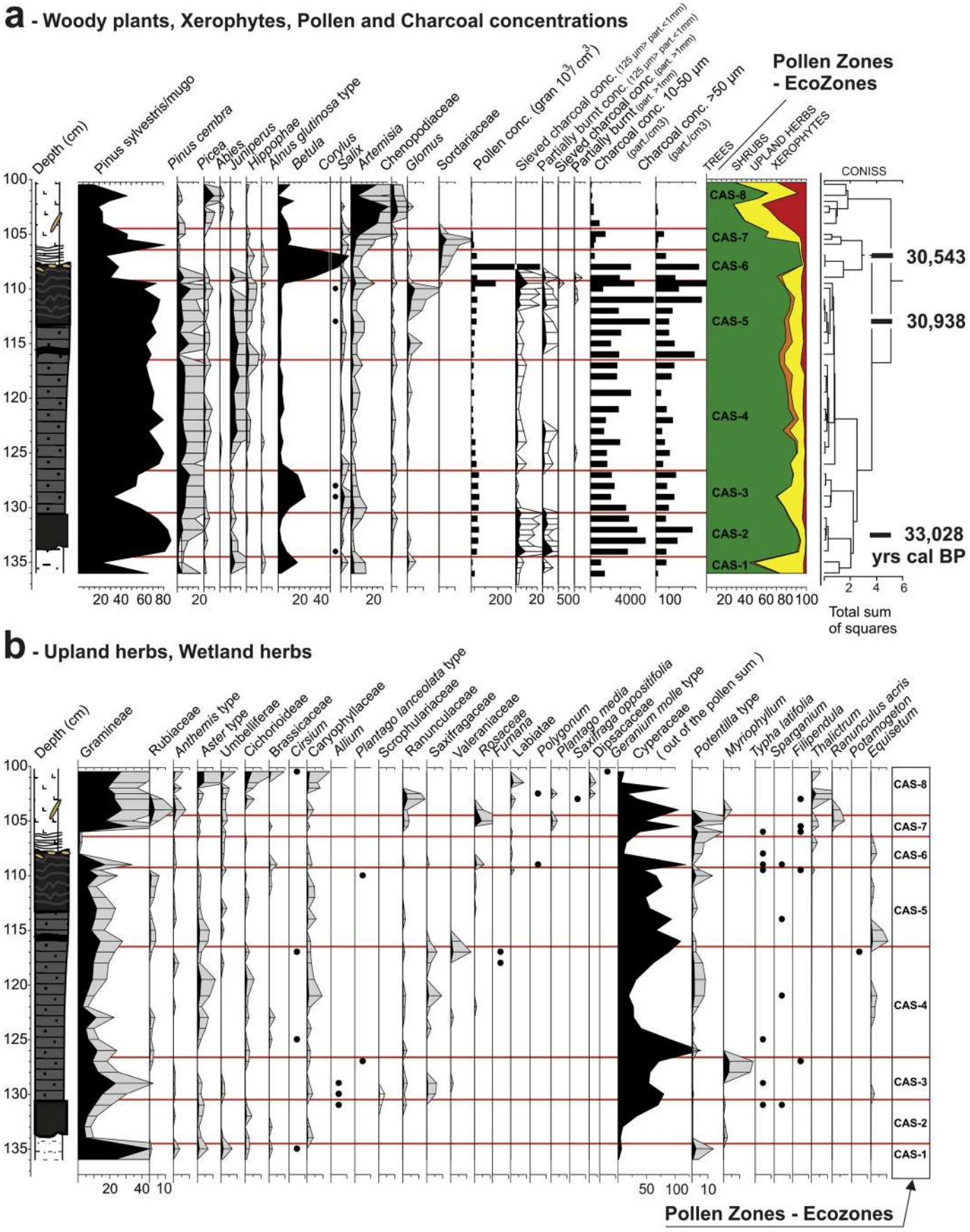

Fig. 7. Palynological and charcoal records. (a) Pollen % of woody plants and xerophytes (*Artemisia*, Chenopodiaceae, *Hippophäe*, *Ephedra*); concentration of pollen and sieved charcoal particles; cumulative pollen diagram and pollen zonation; (b) Pollen % of upland herbs and of wetland and aquatic herbs. The gray curves are plotted with ×5 magnification (×2 for Gramineae). Cyperaceae pollen % have been calculated out of the pollen sum.

3.4. Integrative pollen, charcoal, macrofossil and ecozone stratigraphy

We obtained a pollen and sieved charcoal record with an average sample resolution (133 and 65 years respectively) suitable to detect centennial-scale ecological successions as well as the effects of sub-millennial climate events which characterized the late MIS 3.

The pollen sequence is clustered into eight pollen zones (CAS-1 to 8, Fig. 7). They will be commented in term of ecozones, i.e., taking into consideration proxies of ecological value, available along the stratigraphic zones, such as charcoal, macrofossil content and sedimentary environment. Boundaries of main changes between these ecological proxies broadly correspond to pollen zone clustering (compare Figs. 5, 6,7).

3.4.1. CAS-1 (136–134 cm) – Alluvial environment

Before the onset of organic deposition, sandy sediments are characterized by moderate percentage values of pine (*Pinus sylvestris/mugo),* grass, and other herbs pollen, including sporadic xerophytes (*Artemisia, Ephedra, Hippophaë,* Chenopodiaceae), marking open environments. Pollen deposition in CAS-1 may be affected by floatation. Consequently, plants growing along the channel banks, such as sandy bars, may be overrepresented in this part of the record, together with buoyant pollen such as pine pollen.

3.4.2. CAS-2 (134–130 cm) – Extralocal pine and local birch forests affected by fires

This zone, represented by organic deposits, records peaking pine pollen percentages (*Pinus* tot 75–88%; AP = 85–93%) and abundance of sieved charcoal fragments. The abundances of the sieved macrocharcoal fraction (125 μm–1 mm), along with cm-size fragments (not shown in Fig. 7), suggest that fire affected local environments. Surprisingly enough, wood fragments – i.e. the ones which could be identified to genus level – all belong to cf. *Betula* (Section 3.3, Figs. 5, 6), while the pollen record is dominated by pine. This reflects differences between local components (birch) and extralocal components (pine), which will be discussed in Section 4.2. Indicators of local wetlands are still scanty.

3.4.3. CAS-3 (130–126 cm) – Birch and sedge wetland expansion

A sharp decrease in pine pollen abundance couples with increasing values of *Betula* (birch), the expansion of wetland herb vegetation (Cyperaceae, Gramineae) and increasing micaceous mineral detritus admixed to peat components (lithozone PL4-c, see LOI residue in Fig. 4). The in-situ development of a *Carex* (sedge) fen is shown by the abundance of sedge roots. We infer a withdrawal of extralocal pine forests that had previously been affected by fires, while birches mires and terrestrial wetlands expanded, favored by rising water table.

3.4.4. CAS-4 (126–116 cm) – Extralocal pine forest stand and open xerophytic areas, local sedge mire

Pine pollen increases again (*Pinus* tot. around 70%; AP = 76–90%), together with *Juniperus* and other xerophytes pollen. Cyperacee pollen decreases but sedge peat is still accumulating according to the abundance of roots in sediments. Minerogenic detrital supply remains high (see LOI residue in Fig. 4). Data reconstruct a rather open environment with extralocal pine forest stands, which may have included sporadic spruce, and open land occupied by *Juniperus* and herbs. A treeless sedge mire persists locally, its fluctuations influenced by detrital supply.

3.4.5. CAS-5 (116–109 cm) – Extralocal pine forest stand and open xerophytic areas, expanding local sedge mire

There is a pine pollen stillstand (*Pinus* tot. around 70%; AP = 70–85%), with xerophyte pollen summing up 5–10% (*Juniperus, Artemisia, Hippophäe*); sedge pollen and sedges roots are still abundant in sediments; the minerogenic input decreases. We infer that the sedge fen expanded. In the uppermost zone a new increase of the sieved

Fig. 8. Two different mire communities rich in tree birch in the boreal region. (a) Hummocky bog (*pounnikko* sensu Eurola et al. 1984) in Northern Lapland with tree birch (*B. pubescens* subsp. *tortuosa*) growing on drier mounds (Inari, Lapland, august 2014); (b) Riverside sedge swamp fringing river Ounasjoki with birches growing on tufted sedge mounds (*Carex cespitosa*) (Rovaniemi, Finland, August 2015). Type (b) shares several ecological features with the studied fossil community in N-Italy, i.e. a birch-tall sedge fen fringing a big river, with occasional floods supplying minerogenic detritus.

macrocharcoal fraction (125 μm–1 mm) suggests that recurrent fire affected local environments. A coeval activity of arbuscular mycorrhizal fungi (*Glomus*) point to the development of in situ mycelia, possibly related to nutrients fertilization input by charcoal particles which increased root colonization (Eom et al., 1999).

3.4.6. CAS-6 (109–106 cm) – Fire-induced succession, birch swamp phase (B. pubescens)

Birch pollen massively increased in this zone, mirrored by a decline in pine pollen (*Pinus* tot. 28–39%; AP = 92–97%). Finds of uncharred *Betula* fruits, wood, bark fragments and in situ stumps (Section 4.2) suggest that downy birch occupied the fen, forming a swamp together with tall sedges (*Carex rostrata/vesicaria* achenes) and marsh cinquefoil (*Comarum palustre* achenes and *Potentilla* type pollen), after the CAS-5 fire. Indeed, our fine resolution microbotanical stratigraphy shows that the occurrence of macroscopic charcoal drops down at the CAS-6 onset readily at the level of birch expansion (Fig. 7), suggesting that birch expanded just at the end of a fire phase.

3.4.7. CAS-7 (106–104 cm) – Burial of the peat mire by flooding

Three pollen samples at the upper boundary of the peat layer show the decline of pollen from all forest components (AP = 28–60%) and expanding herb wetlands (Cyperaceae, Gramineae p.p., *Potentilla* type pollen and *Comarum palustre* achenes, *Thalictrum* pollen). This change happens just over the contact peat/silt representing the burial of the peat mire after a flood (Section 4.1, Fig. 3g).

3.4.8. CAS-8 (104–100 cm) – Expansion of xerophytic grasslands and unvegetated fields

This zone is marked by sharp rise of *Artemisia* pollen and of several upland herbs typical for xerophytic grasslands and poorly vegetated fields such as dry river floors and/or semideserts. The Arboreal Pollen is reduced to values (20–30%) characteristic for open landscapes.

4. Discussion

4.1. The sedimentary environment

The peat layer studied in the present work formed in a long-lasting wetland occupied by a mire and finally by a swamp forest, fed by minerogenic silt, in the sandy floodplain of the Adda River valley (Ravazzi et al., 2012). The wetland area most probably originated as an abandoned river channel, around 33 kyr cal BP (zone CAS-1), and it was first pioneered by a terrestrial forest (locally birch, with pine in the surroundings) but soon developed as a peat basin. Peat accumulation lasted about 2500 yr, until the mire was buried by a major flooding. The relatively stable sedimentary environment in this time span requires an overall subsurface water saturation, favored by a thin-grained texture (silty sands) and excludes high-energy fluvial dynamics and aggradation processes in the area, which would have implied an immediate wetland burial by minerogenic fluvial sediments.

We first reconstruct the wetland birch-sedge plant community; then, we discuss the interplay between environmental history, fire regime and climate changes.

4.2. The birch-sedge plant community

The only interval providing adequate macrofossil preservation to identify several components of plant community is zone CAS-6, from the topmost peat layer, i.e., the birch swamp community. *Betula* pollen becomes dominant in this zone, in agreement with the identification of *Betula pubescens* group as the main in-situ growing birch species, documented both from stump bark features (Section 3.2) and from fruits and wood (Section 3.3). The fruits record indicates that *B. pendula* was an accessory species, while dwarf birch *B. nana and B. humilis* are absent. So far there is only circumstantial evidence about the occurrence of dwarf birches south of the Alps (Schneider and Tobolski, 1985; Monegato et al., 2015). A small increase of *Alnus glutinosa* type pollen (incl. *A. incana*), with very low % values in zone CAS-6, is not considered significant of its occurrence in the wetland, as there are neither alder fruits nor wood. The peat consists mostly of woody plant remains, but

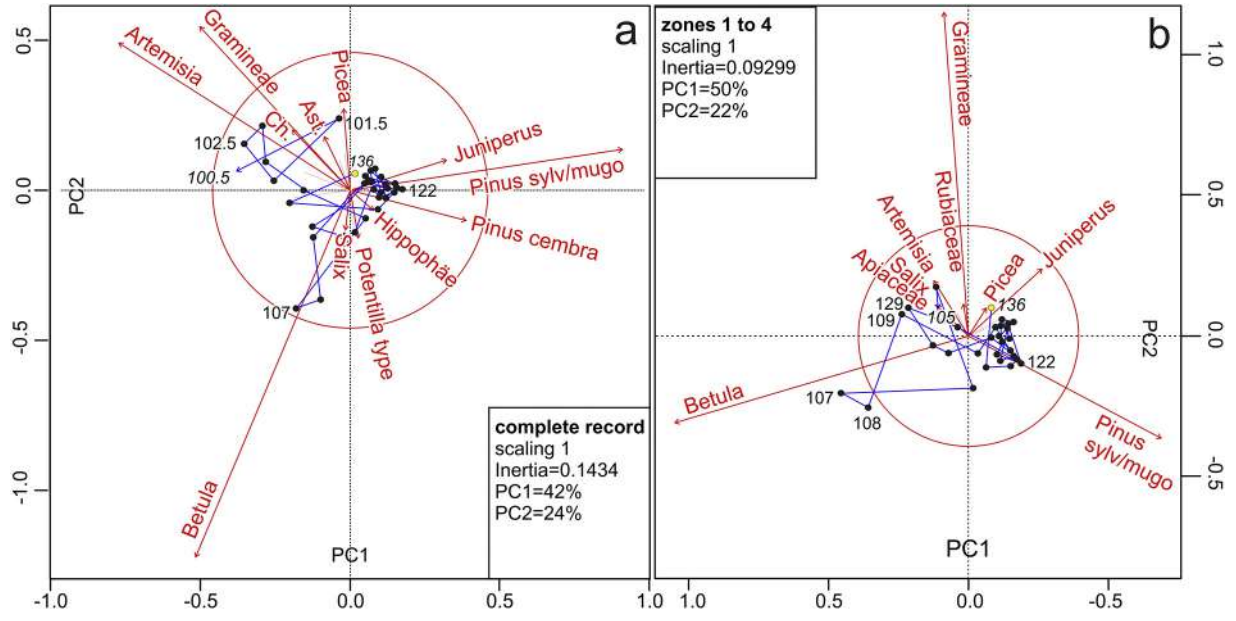

Fig. 9. Comparison of variance explained by the first two PCA axes in (9a) the whole Casaletto pollen record and (9b) in the pine-dominated interval (scaling 1 – circle of equilibrium contribution). The paleoecological succession from base record (136) to top (100.5) is shown by connecting distances among sample levels. A few sample labels mark the main directions observed along the succession. Biological variables with eigenvalues close or exceeding the circle of equilibrium are labeled together with selected taxa having lower pollen variation abundances but important as ecological indicators. Cyperaceae have been excluded from the analyzed variance (see text).

actually contains rhizome, stem and root fragments of herbs (Suppl. Table 2) which belong to the Cyperaceae family (sedge), among which the tall sedge *Carex rostrata/vesicaria* (Suppl. Table 1 and Fig. 6o). Nevertheless, sedge pollen abundance decreases in the CAS-6 acme event of birch pollen expansion, suggesting plant belting along the swamp pedobiome ecotone, with birch occupying a niche on the terrestrial swamp belt, and *C. rostrata/vesicaria* on surface-water influence, on higher floodwater levels.

Today, this community is completely unknown for S-Europe, and extremely rare in the subalpine belt of the Alps (Ellenberg, 1988). It appears that all the identified fossil species still occur in the boreal belt in the Central Alps, but do not co-occur in the same community. The helophyte and hygrophilous herbs *Carex rostrata/vesicaria*, *Comarum palustre* and *Filipendula ulmaria* still occurred in the central Po Plain at the beginning of the nineteenth century, while *B. pubescens* is missing in the whole N-Italian plain (Jalas and Suominen, 1987; Martini et al., 2012).

On the other hand, the described fossil plant combination has several comparisons with contemporary western-to-central European mires and also with eastern European and Siberian bogs (Eurola et al., 1984; Oberdorfer, 1977; Walter and Breckle, 1986, Rodwell, 1995; Hytteborn et al., 2005, see Fig. 8b). This allows further ecological and ecoclimatic inferences, here briefly discussed. The wooded mires with *B. pubescens* and tall sedges are very common in Fennoscandia, being recognized as a mire type (the so-called *Betula pubescens* swamp) which characterize minerogenic water and areas with periodic flooding (Kalliola, 1973; Eurola et al., 1984). *B. pendula* does not take part in these swamp communities, not even in the oceanic warm temperate region of Western Europe (Rodwell, 1995). Indeed, *B. pubescens* has a much higher tolerance to high soil water content (Hytteborn et al., 2005). In Central Europe, *B. pubescens* replaces alder carr (*Alnus glutinosa*) in the poor base fen (Ellenberg, 1988), a circumstance that recalls the low to moderate carbonate amount characterizing the sediment petrography carried by the Adda River (Vezzoli and Garzanti, 2009). On the other hand, the absence of alder in the studied peat may depends on climate pattern characterizing the northern Italian plains during the late MIS 3 stadial-interstadial sequence (GI8–GI5, Rasmussen et al., 2014) before the onset of the Heinrich Stadial 3 (HS3) and the Last Glacial Maximum, with July temperatures not exceeding 15 °C which excluded all warm-temperate tree species from the forest biome (Pini et al., 2010; Monegato et al., 2015; Badino et al. 2020a, 2020b). The current altitudinal limit of *A. glutinosa* in the Alps does not reach 1200 m a.s.l., being frequently replaced by *A. incana* on coarse gravelly alluvial deposits (Ellenberg, 1988). This is because *A. incana* requires fluctuating ground water levels (Fremstad, 1981; Hytteborn et al. 2005), thus it is currently absent from the fine-grained, poorly oxygenated central plains in northern Italy (Jalas and Suominen 1987; Svenning & Skov 2004). On its northern boreal limit, *A. glutinosa* reaches to the boreonemoral belt (Moen 1999), while *A. incana* extends further north in the mixed boreal forest until the arctic timberline, locally admixing with *B. pubescens* into the arctic birch formations (Kalliola, 1973; Moen 1999). In W-Siberia, these communities are found in periodically overflooded mires along the Ob River, anoxic, with gley formation in deeper horizons (Walter and Breckle 1986).

The *Betula pubescens* group – tall sedges swamp community is here described for the first time in deposits from the last glaciation in the northern Italian plain. It is concluded that this woody mire type developed in a floodplain mire, i.e., in a flooded, anoxic fen, fed by waters with poor-carbonate suspended load, under a boreal climate which excluded warm-temperate trees. Alders were also excluded from dominant trees in this pedobiome, most probably due to a combination of cool climate and thin soil texture. Anoxic conditions favored *B. pubescens* group, as predicted by its modern ecology, in view of its ability to enhance gas exchange through the development of bark lenticels. The dynamic relationships between birch swamp and fire will be discussed in the next section.

4.3. The environmental history and the ecological succession induced by forest fires

The PCA ordination on pollen variables addresses the analysis of main changes driving the vegetation dynamics in the interval of peat accumulation (CAS 1–6, Fig. 9b) and in the complete record, i.e., including the final event of burial by flooding and *Artemisia* expansion (CAS 1–8, Fig. 9a). We remark here that Cyperaceae pollen abundance, showing large variations, is related to the local mire. Sedge pollen was excluded both from the pollen sum and from the variance analyzed in Fig. 9.

During the phase of stable wetland swamp (CAS 1–6, Fig. 9b) grass pollen abundance on PCA axis 1 and the opposition between birch pollen and conifer pollen on PCA axis 2 explain much of the total variance. High covariation between Gramineae and Cyperaceae pollen curves is evident from a simple visual inspection of the pollen diagram (Fig. 7). This suggests that grasses and sedges were both related to the local mire dynamics; thus, we infer that PCA axis 1 represents the dynamics of the local herb mire. Pollen variations of woody plants are not involved in this variance direction. Most probably birches and conifers were settling drained terrestrial environments. The opposition between birch and pine on axis 2 is clearly related to an ecological progression from pine to birch, which is induced by forest fire, as shown by the record of sieved charcoal fractions (Figs. 4 and 7, see description CAS 6 in Section 3.4.6). Birch expansion (acme at labeled samples 129 and 107 in Fig. 9b) started at the very end of fire phases. This is a well-known feature in circumboreal and temperate oceanic forest ecosystems; indeed, an early birch phase is characteristic of fire-induced successions in mixed coniferous forests (Atkinson 1992; Schulze et al. 2005). Fire can easily kill mature birch, but surviving birches produce stress seed crops and fire-related sprouting (Perala and Alm 1990; Masaka 2000) to enable fast regeneration. A fire-induced birch-to-pine cycle is repeated twice along the 2500 years-time span covered by the peat layer. Fire produced just a slight arboreal decrease along zones CAS 1–6 (see cumulative AP curve in Fig. 7). Open land did not expand in these zones despite the fires.

4.4. Heinrich Stadial 3 and the flood event burying the birch swamp

The end of the birch mire – forming the uppermost peat layer – was due to an intriguing event of flooding whose accurate age matches a major event in the millennial scale climate variability characterizing the last glaciation. Hereafter, we examine the paleocological and chronostratigraphic evidence of environmental and climatic change associated with the peat/silt boundary. Besides, we point to the climate teleconnections with the Atlantic Ocean.

The stratigraphic framework of the peat-to-silt contact is shown in Fig. 3. Decimetric-scale undulations (Fig. 3h) and apparent convolutions (Fig. 3d) remark a hummocky microtopography supporting birch stumps rooted on small mound tops (see birch stems and a stump marked by w1–w2–ws in Fig. 3d and h; see also Fig. 5a, b). Hollows filled by alternating peat and silt laminae (PL5/6 in Fig. 3h) represent cyclic organic and minerogenic deposition at the burial event onset. Hummocky birch swamps and bogs are widespread and well-studied in all the circumboreal region (e.g., Kalliola, 1973; Walter and Breckle 1986, Fig. 9). Their development may depend on microhabitat differentiation due to plant structures (tree-rooting system on Ericaceae-hummocks or on sedge tussocks, Fig. 8b: see Eurola et al. 1984). In the northern boreal zone, Ericaceae-hummocks may be related to the development of seasonal frost (e.g., in the *pounnikko* bogs in Fennoscandia, Fig. 8a; Walter 1968; Eurola et al., 1984), or to a combined effect. Cryoturbation or other permafrost features are not diagnostic factors in these microscale landforms (Seppälä 1997). The studied fossil peat layer contains woods which are related to sedge tussocks, suggesting that small-scale topographic mounds were produced by tree-rooting system action, then compressed by sediment load. This microscale deformation does not require an action of permafrost. On the other hand, the observed

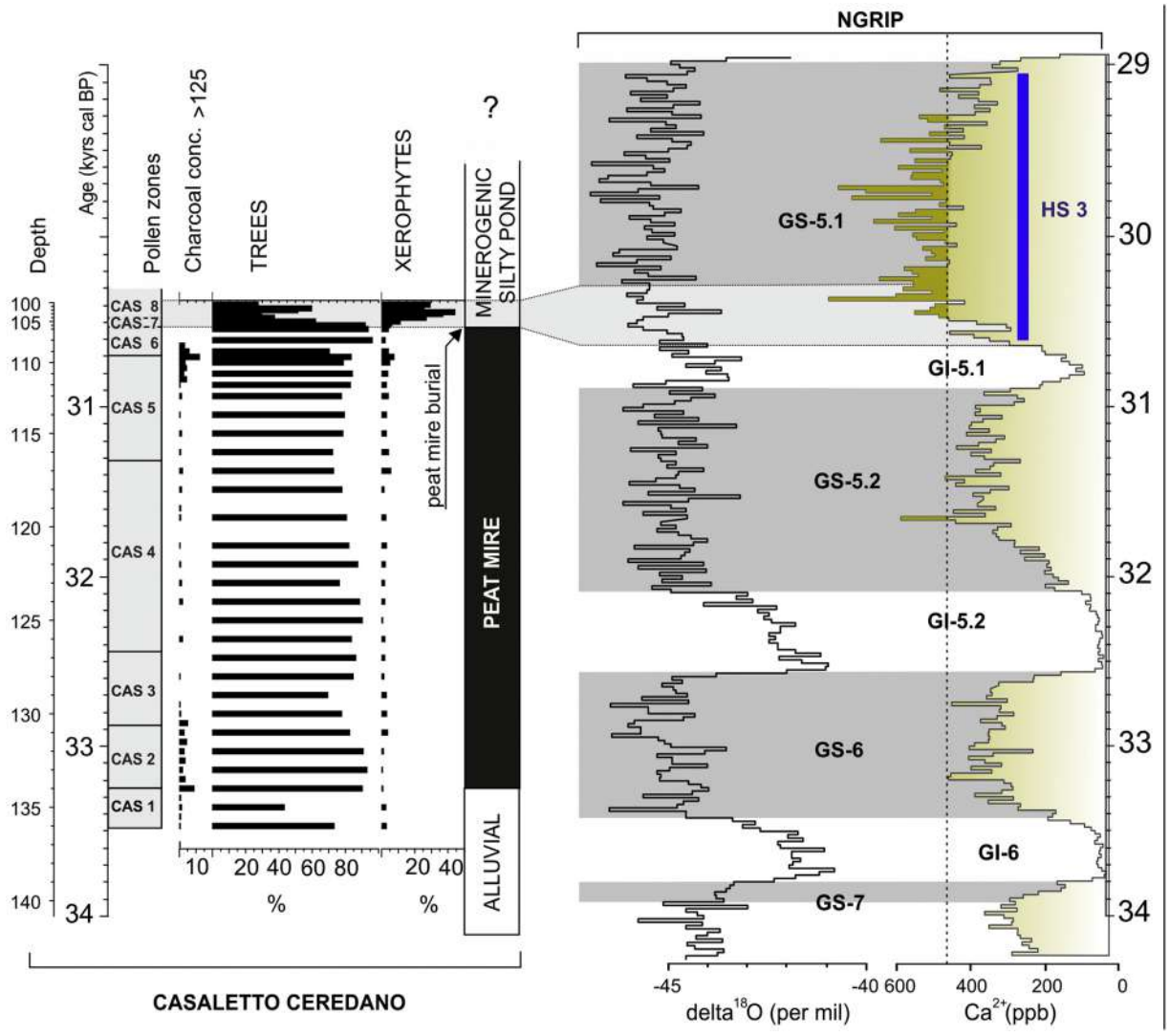

Fig. 10. Chronostratigraphic framework, summary paleobotanical proxies (Arboreal Pollen; sum of xerophytes – i.e., *Artemisia, Ephedra*, Chenopodiaceae, *Hippophäe*; sieved charcoal) compared with the isotopic record and Ca^{2+} dust proxy from the NGRIP core (from Rasmussen et al. 2014). The NGRIP data have been 20-yr averaged. An empiric threshold has been traced at 460 ppb Ca^{++} to show a GS 5.1. maximum much more pronounced than in previous stadials GS-6 and GS-5.2. The proposed correlation of the HS3 with the GI 5.1 is supported by consistent NGRIP chronology (GICC05) and Atlantic Ocean chronologies through correlation of rapid climate changes at stadial/interstadial limits (Waelbroeck et al. 2019).

geometry of the peat-to-silt contact excludes hiatuses or erosional phases at the time of the burial. We argue that the age obtained on wood outer rings of the birches rooted on hummocks may provide an accurate age for the burial event. The radiocarbon measurements of two samples (w1 and w2 in Fig. 3h) were pooled in order to reduce the measurement uncertainty. The pooled age (30,405–730/+559 yr cal BP (pooled age median probability and 2σ uncertainty; modeled pooled median 30,543 yr cal BP; Table 1) is considered to date the birch death, slightly older than the age of the embedding silt.

The paleoecological record from the silt layer (Fig. 7 samples 106–100.5 cm) diverges from the *Pinus-Betula* succession above described (Section 4.3), in that pollen of open land communities sharply expands (*Artemisia, Ephedra*, Chenopodiaceae, *Hippophäe* and upland herbs). Upland biological descriptors of open vegetation strongly increase the PCA variance (inertia from 0.092 to 0.14) pointing in the upper left of the biplot (Fig. 9a). Question now is whether the observed change towards drought-adapted open ecosystems in the upland area may be predicted by direct impact of climate change on vegetation, or by the local sedimentary environment dynamics (from wetland to minerogenic alluvial), or by a multifactorial triggering. The withdrawal of pine forests and their replacement by grasslands and semideserts in the upland area is best explained by a significant increase in continentality affecting the regional climate of the northern Italian alluvial plains around 30,497 ± 594 yr cal BP (2σ uncertainty). On the other hand, the observed enhanced river activity may also have contributed to the development of open areas, such as open drylands on sandy river channels and bars, providing a positive feedback to forest withdrawal. This figure may appear controversial if analyzed at local scale, as increasing dryness should not enhance river discharge, so it deserves to be addressed in the light of the global climate events occurred at 30.5 kyr cal BP.

Teleconnections with the Atlantic and Arctic framework of the stadial–interstadial climate variability between 34 and 29 kyr cal BP are examined in Fig. 10. The interstadial climates experienced during GI-6, GI-5.2 and GI-5.1 may have enhanced forest biomass and local fire spread, as it is observed in the nearby record of the Fimon Lake in N-Italy (location in Fig. 1; Badino et al., 2019 and in review). Nevertheless, open areas did expand neither after the fire phases, nor during stadials GS-6 and GS-5.2. Overall, between 33 and 30.5 kyr cal BP the central Po Plain was affected by a cold temperate regional climate of middle boreal type (Moen 1999) with Tjuly < 15 °C, but well within the climatic woodland limits (see Section 4.2). Conversely, at 30.5 kyr

cal BP we observed a sharp ecosystem change and we claimed an important increase in climate continentality. The uppermost age available from the Casaletto Ceredano section fits the modeled age of the Heinrich Stadial 3 onset at nearby site of Fimon Lake (30,400 ± 860 yr cal BP, Badino et al., in review, see Fig. 1), and the onset of GS-5.1 in the Greenland ice event chronology (30,600 ± 1008 yr cal BP, Rasmussen et al. 2014, see Fig. 10). The Heinrich Stadial 3 in the North Atlantic triggered reorganization of the atmospheric circulation at hemispheric scale, desertification of the continental Asia, and consequent peaks of dust accumulation in the Greenland ice (Fischer et al. 2007), more pronounced than in previous stadials GS-6 and GS-5.2 (see Ca^{++} curve in the NGRIP record plotted in Fig. 10). The observed environmental changes correspond to a lockdown of moist westerlies and of their Rossby waves in W-Mediterranean due to southern displacement of the Intertropical Convergence Zone (ITCZ), causing substantial continentalization at the onset of Heinrich Stadial 3 (Sanchez-Goni et al., 2008; Fleitmann et al. 2009).

The climate teleconnection so far discussed points to an allogenic forcing of the flooding phase sealing the peat, i.e., of the Heinrich Stadial 3 onset, acting both on ecosystems and indirectly on the river dynamics of the Po Plain. Auto-cyclic geomorphic processes (e.g., a lateral shift of the river channel that reactivates a stable portion of the floodplain) would hardly have affected the entire pollen source area. Furthermore, the peaks of xerophytic plants pollen growing in semidesert biomes or pedobiomes does not occur in the minerogenic alluvial deposition underlying the organic deposition cycle (i.e., basal pollen zone CAS-1). Increased river discharge and minerogenic load may have been driven by increased discharge and detrital supply from the eastern lobe of the advancing Adda Glacier at the onset of Heinrich Stadial 3. Indeed, the studied site is located in the lower megafan belt of the Adda River, representing the distal sandur of the Adda Glacier (see Fig. 1b for megafan area and the maximum position reached by the Adda Glacier). Here, summertime meltwater discharge is accompanied by intense outbursts affecting large megafan areas, distal to the glacial front, and these events produce large floods even in cold semiarid regions (i.e. jökulhaup-type flood deposits, Benn and Evans, 2010). We are aware that the front position of the eastern lobe of the Adda glacier at 30.5 kyr cal BP isn't known yet; still, we speculate that the event of peat sealing could be produced by early fluvioglacial outbursts in the central Po Plain, pre-dating by some 4 kyr the culmination of glaciers in their piedmont amphitheaters, which is currently dated to 26 kyr cal BP (Monegato et al., 2007).

From a strict chronostratigraphic approach, the sedimentary record here presented spans the onset of the Late Würm in the Alpine regional chronostratigraphy (Spötl et al. 2013), while pre-dating the Last Glacial Maximum (onset at about 27 kyr cal BP, Clark et al., 2009; Hughes and Gibbard, 2015; Monegato and Ravazzi, 2018).

5. Conclusions

This study provided insight about plant communities settling the Central Po Plain just before the onset of the Last Glacial Maximum, between 33 and 30.5 kyr cal BP. The discovery of datable wood and cm-sized charcoal fragments in several levels of a peat section is of major relevance for the chronology of the last glaciation as it allows for precise AMS dating on undecayed lignine.

A *Betula pubescens* group – tall sedge swamp fossil community is described for the first time in the southern Alpine foreland, on the base of multiple microbotanical and macrobotanical evidence. This woody mire type developed in the floodplain of a major Alpine river as an anoxic fen, flooded by waters with poor-to-moderate carbonate suspended load. The local anoxic conditions in the swamp fringing the river favored *B. pubescens* group, the downy birch, as predicted by its ability to enhance gas exchange through development of bark lenticels. Upland areas were occupied by pine woodlands with only limited patches of open vegetation. The reconstructed climate compares to northern boreal zone, with Tjuly <15 °C, excluding warm-temperate trees. Alders (*Alnus* sspp.) were also excluded from dominant trees in this pedobiome, most probably due to a combination of cool climate and thin soil texture.

The dynamic of the birch swamp is found to relate to fire periods. A fire-induced birch-to-pine cycle is repeated twice along the 2500 years-time span covered by the peat layer. Fire produced just a slight arboreal decrease, as open land did not expand during the time spanned by these pollen zones (33–30.5 kyr cal BP) and regardless of the intervening stadial–interstadial cycles.

The swamp was finally buried by a major flood. This event is precisely dated to 30,497 ± 594 yr cal BP (2σ uncertainty), thanks to finds of in situ birch sumps and stems populating the sedge-hummocky wetlands, sealed by minerogenic silt. We argued that a significant increase in continentality affected the regional climate of the northern Italian alluvial plains, causing the withdrawal of upland pine forests and their replacement by grasslands and semideserts. Autocyclic processes, or local edaphic effects related to the river dynamics, may have added feedback to the observed ecosystem change, but we argued for an external (climatic) trigger. Based on teleconnections with the Atlantic and Arctic framework of the stadial-interstadial climate variability, these changes can be consistently related to a lockdown of moist westerlies intervening with the onset of Heinrich Stadial 3.

Author contributions

C.R. designed the work. M.D. coordinated field work, in situ measurements and section sampling. M.De A. realized spatial elaborations. F.B., P.B., M.D. L.G., MD.N. and Ro.P. carried out the microbotanical study, LOI and the sieved charcoal analysis. Re.P. studied plant macroremains (wood anatomy, fruits and seeds). C.R. analyzed the structure of fossil bark. C.R. wrote the paper. All authors shared the ideas of the paper, discussed the environmental and chronostratigraphic assessment, and reviewed earlier drafts of the manuscript. The revisions by two anonymous referees were greatly appreciated.

Declaration of Competing Interest

The authors declare that they have no known competing financial interests or personal relationships that could have appeared to influence the work reported in this paper.

Acknowledgments

The financial support by Banca Popolare di Crema to radiocarbon dating of the Casaletto Ceredano samples is gratefully acknowledged. Thanks are due to the colleagues of the group currently co-working on Paleogeographic Map of the Great Adriatic-Padanian Region for the permission to extract the yet unpublished base of Fig. 1b (Davide Margaritora and Marco Peresani, Univ. of Ferrara; Mattia de Amicis, Univ. of Milano Bicocca; Roberta Pini and Cesare Ravazzi, CNR-IGAG; Alessandro Fontana and Paolo Mozzi, Univ. of Padova; Giovanni Monegato, CNR-IGG, Padova; Andrea Zerboni, Univ. of Milano). Stefano Armiraglio (Museo di Scienze Naturali di Brescia) adviced on the modern native range of sedges and birches in N-Italy. This is a contribution to the CNR-IGAG research line DTA.AD001.112 – Quaternary paleoenvironments and paleoclimate.

Appendix A. Supplementary data

Supplementary data to this article can be found online at https://doi.org/10.1016/j.revpalbo.2020.104276.

References

Atkinson, M.D., 1992. *Betula pendula* Roth (*B. verrucosa* Ehrh.) and *B. pubescens* Ehrh. J. Ecol. 80 (4), 837–870.

Badino, F., Pini, R., Ravazzi, C., Arrighi, S., Bertuletti, P., Bortolini, E., Figus, C., Lugli, F., Marciani, G., Margaritora, D., Oxilia, G., Romandini, M., Benazzi, S., 2019. Sub-millennial scale variability between Heinrich events 4 and 3 in the long terrestrial paleoecological archive of Lake Fimon (northeastern Italy). XX Congress INQUA, Dublin.

Badino, F., Pini, R., Ravazzi, C., Margaritora, D., Arrighi, S., Bortolini, E., Figus, C., Giaccio, B., Lugli, F., Marciani, G., Monegato, G., Moroni, A., Negrino, F., Oxilia, G., Peresani, M., Romandini, M., Ronchitelli, A., Spinapolice, E., Zerboni, A., Benazzi, S., 2020a. An overview of Alpine and Mediterranean palaeogeography, terrestrial ecosystems and climate history during MIS 3 with focus on the Middle to Upper Palaeolithic transition. Quat. Int. in press.

Badino, F., Pini, R., Bertuletti, P., Ravazzi, C., Margaritora, D., Delmonte, B., Monegato, G., Reimer, P.J., Vallè, F., Maggi, V., Arrighi, S., Bortolini, E., Figus, C., Lugli, F., Marciani, G., Oxilia, G., Romandini, M., Silvestrini, S., Benazzi, S., 2020b. The fast-acting "pulse" of Heinrich stadial 3 in a mid-latitude boreal ecosystem: ecoclimatic patterns and fire regimes. Scient. Rep. submitted, In press.

Benn, D.I., Evans, J.A., 2010. Glaciers and glaciation 2nd ed. Routledge, London.

Berggren, G., 1969. Atlas of seeds and small fruits of Northwest European plant species with morphological descriptions. Part 2 Cyperaceae. Swedish Natural Science Research Council, Lund.

Berglund, B., Digerfeldt, G., 1970. A palaeoecological study of the Late-Glacial Lake at Torreberga, Scania, South Sweden. Oikos 21 (1), 98–128. https://doi.org/10.2307/3543845.

Beug, H.J., 2004. Leitfaden der Pollenbestimmung für Mitteleuropa und angrenzende Gebiete. Verlag Dr. Friedrich Pfeil, München, Germany.

Bialobrzeska, M., Trnchanowiczrwna, J., 1960. The variability of shape of fruits and scales of the European birches (*Betula* L.) and their determination in fossil materials. Monogr Bot (Warszawa) 9 (2), 1–93.

Birks, H.H., 2007. Plant macrofossil introduction. In: Elias, S.A. (Ed.), Encyclopedia of Quaternary Science. Volume 3. Elsevier, Amsterdam, pp. 2266–2288.

Bojňanský, V., Fargašová, A., 2007. Atlas of seeds and fruits of Central and East-European flora. The Carpathian Mountains Region. Springer, Dordrecht.

Bronk Ramsey, C., 2017. Methods for summarizing radiocarbon datasets. Radiocarbon 59 (2), 1809–1833.

Butler, B.T., 1909. The western American birches. Bull. Torrey Bot. Club 36 (8), 421–440.

Cappers, R.T.J., Bekker, R.M., Jans, J.E.A., 2006. Digitale Zadenatlas van Nederland (Digital Seed Atlas of The Netherlands). Groningen Archaeological Studies 4. Barkhuis Publishing, Eelde.

Carcaillet, C., Blarquez, O., 2017. Fire ecology of a tree glacial refugium on a nunatak with a view on Alpine glaciers. New Phytol. 216 (4). https://doi.org/10.1111/nph.14721.

Caudullo, G., de Rigo, D., 2016a. *Populus tremula* in Europe: Distribution, habitat, usage and threats. In: San-Miguel-Ayanz, J., de Rigo, D., Caudullo, G., Houston Durrant, T., Mauri, A. (Eds.), European Atlas of Forest Tree Species. Publ. Off. EU, Luxembourg, pp. 138–139.

Caudullo, G., de Rigo, D., 2016b. *Populus alba* in Europe: Distribution, habitat, usage and threats. In: San-Miguel-Ayanz, J., de Rigo, D., Caudullo, G., Houston Durrant, T., Mauri, A. (Eds.), European Atlas of Forest Tree Species. Publ. Off. EU, Luxembourg, pp. 134–135.

Clark, J.S., 1988. Particle motion and the theory of charcoal analysis: Source area, transport, deposition, and sampling. Quat. Res. 30 (1), 67–80.

Clark, P.U., Dyke, A.S., Shakun, J.D., Carlson, A.E., Clark, J., Wohlfarth, B., Mitrovica, J.X., Hostetler, S.W., McCabe, A.M., 2009. The Last Glacial Maximum. Science 325, 710–714.

Crawford, R.M.M., 2014. Tundra-Taiga Biology. Oxford University Press, Oxford.

Davolio, S., Volonte, A., Manzato, A., Pucillo, A., Cicogna, A., Ferrario, M.E., 2016. Mechanisms producing different precipitation patterns over North-Eastern Italy: Insights from HyMeX-SOP1 and previous events. Q. J. R. Meteorol. Soc. 142, 188–205.

Ellenberg, H., 1988. Vegetation Ecology of Central Europe. Cambridge University Press, Cambridge.

Enache, M.D., Cumming, B.F., 2007. Charcoal morphotypes in lake sediments from British Columbia (Canada): An assessment of their utility for the reconstruction of past fire and precipitation. J. Paleolimnol. 38, 347–363.

Eom, A.H., Hartnett, D.C., Wilson, G.W.T., Figge, D.A.H., 1999. The effect of fire, mowing and fertilizer amendment on arbuscular mycorrhyzas in tallgrass prairie. Am. Midl. Nat. 142 (1), 55–70.

Eurola, S., Hicks, S., Kaakinen, E., 1984. Key to Finnish mire types. ed. In: Moore, P. (Ed.), European Mires. Academic Press, London, pp. 11–117.

Evert, R.F., 2006. Esau's Plant Anatomy, Meristems, Cells, and Tissues of Ther Plant Body: Their Structure, Function, and Development. 3rd edn. Wiley & Sons, New Jersey.

Farrar, J.L., 1995. Trees of the Northern United States and Canada. Iowa State University, Iowa.

Finsinger, W., Schwörer, C., Heiri, O., Morales-Molino, C., Ribolini, A., Giesecke, T., Haas, J.N., Kaltenrieder, P., Magyari, E.K., Ravazzi, C., Rubiales, J.M., Tinner, W., 2018. Fire on ice and frozen trees? Inappropriate radiocarbon dating leads to unrealistic reconstructions. Comment on Carcaillet & Blarquez (2017) 'Fire ecology of a tree glacial refugium on a nunatak with a view on Alpine glaciers'. New Phytol. https://doi.org/10.1111/nph.15354.

Fischer, H., Siggaard-Andersen, M.-L., Ruth, R., Rothlisberger, R., Wolf, E., 2007. Glacial/interglacial changes in mineral dust and sea-salt records in polar ice cores: Sources, transport, and deposition. Rev. Geophys. 45 (1).

Fleitmann, D., Cheng, H., Badertscher, S., Edwards, R.L., Mudelsee, M., Göktürk, O.M., Fankhauser, A., Pickering, R., Raible, C.C., Matter, A., Kramers, J., Tüysüz, O., 2009. Timing and climatic impact of Greenland interstadials recorded in stalagmites from northern Turkey. Geophys. Res. Lett. 36 (19), 1–5. https://doi.org/10.1029/2009GL040050.

Fontana, A., Mozzi, P., Marchetti, M., 2014. Alluvial fans and megafans along the southern side of the Alps. Sediment. Geol. 301, 150–171.

Fremstad, E., 1981. Flommarksvegetasjon ved Orkla. Sør-Trøndelag. Gunneria 38, 1–80.

Freund, H., Birks, H.H., Birks, H.J.B., 2001. The identification of wingless Betula fruits in Weichselian sediments in the Gross Todtshorn borehole (Lower Saxony, Germany) - The occurrence of Betula humilis Schrank. Veg. Hist. Archaeobot. 10 (2), 107–115.

Gardiner, A.S., 1958. Variation in bark characteristics in birch. Scott. For. 12 (4), 191–195.

Grimm, E.C., 2015. Tilia/tgview 2.0.41. Illinois State Museum, Research and Collections Center, Springfield, IL.

Harrison, S.P., Prentice, I.C., 2003. Climate and CO_2 controls on global vegetation distribution at the last glacial maximum: Analysis based on palaeovegetation data, biome modelling and palaeoclimate simulations. Glob. Chang. Biol. 9 (7), 983–1004.

Harrison, S.P., Sanchez Goñi, M.F., 2010. Global patterns of vegetation response to millennial-scale variability and rapid climate change during the last glacial period. Quat. Sci. Rev. 29, 2957–2980.

Hippe, K., Fontana, A., Hajdas, I., Ivy-Ochs, S., 2018. A high-resolution ^{14}C chronology tracks pulses of aggradation of glaciofluvial sediment on the Cormor megafan between 45 and 20 ka BP. Radiocarbon 60 (3), 1–18.

Hosch, S., Zibulski, P., 2003. The influence of inconsistent wet-sieving procedures on the macroremains concentration in waterlogged sediments. J. Archaeol. Sci. 30, 849–857.

Hughes, P.D., Gibbard, P.L., 2015. A stratigraphical basis for the last glacial maximum (LGM) -. Quater. Internat. 383, 174–185.

Hynynen, J., Niemistö, P., Viherä-Aarnio, A., Brunner, A., Hein, S., Velling, P., 2010. Silviculture of birch (*Betula pendula* Roth and *Betula pubescens* Ehrh.) in northern Europe. Forestry 83 (1), 103–119. https://doi.org/10.1093/forestry/cpp035.

Hytteborn, H., Maslov, A.A., Nazimova, D.I., Rysin, L.P., 2005. Boreal forests of Eurasia. In: Andresson, F. (Ed.), Coniferous Forests. Ecosystems of the Worlds. 6, pp. 23–99.

Jacquiot, C., Trenard, Y., Dirol, D., 1973. Atlas d'Anatomie des Bois des Angiosperms. Centre Technique du Bois, Paris.

Jalas, J., Suominen, J. (Eds.), 1987. Atlas Florae Europaeae. II. Salicaceae to Balanophoraceae. Cambridge University Press, Cambridge.

Jensen, K., Lynch, E.A., Calcote, R., Hotchkiss, S.C., 2007. Interpretation of charcoal morphotypes in sediments from Ferry Lake, Wisconsin, USA: Do different plant fuel sources produce distinctive charcoal morphotypes? Holocene 17, 907–915.

Kaplan, J.O., Pfeiffer, M., Kolen, J.C.A., Davis, B.A.S., 2016. Large scale anthropogenic reduction of forest cover in Last Glacial Maximum Europe. PLoS One 11 (11). https://doi.org/10.1371/journal.pone.0166726.

Kats, N.Y., Kats, S.V., Kipiani, M.G., 1965. Atlas and Key to Identification of Fossil Fruits and Seeds Occurring in the Quaternary Deposits of the USSR. Nauka, Moscow (in Russian).

Kozlowski, T.T., 2012. Shedding of Plants Parts. Elsevier, Amsterdam.

Lambeck, K., Roubya, H., Purcell, A., Sun, Y., Sambridge, M., 2014. Sea level and global ice volumes from the Last Glacial Maximum to the Holocene. PNAS 111 (43), 15296–15303.

Lane, S.N., Borgeaud, L., Vittoz, P., 2016. Emergent geomorphic–vegetation interactions on a subalpine alluvial fan. Earth Surf. Process. Landforms 41, 72–86.

Luetscher, M., Boch, R., Sodemann, H., Spötl, C., Cheng, H., Edwards, R.L., Frisia, S., Hof, F., Müller, W., 2015. North Atlantic storm track changes during the Last Glacial Maximum recorded by Alpine speleothems. Nat. Comm. 6(264).

Martinetto, E., Bouvet, D., Vassio, E., Magni, P., Jiménez-Mejías, P., 2014. A new protocol for the collection and cataloguing of reference material for the study of fossil Cyperaceae fruits: The Modern Carpological Collection. Rev. Palaeobot. Palynol. 201, 56–74.

Martini, F., Bona, E., Federici, G., Fenaroli, F., Perico, G., 2012. Flora Vascolare della Lombardia centro-orientale. parte generale vols. 1. Lint, Trieste.

Masaka, K., 2000. McVean, D.N., 1956. Ecology of *Alnus glutinosa* (L.) Gaertn: IV. Root System. J. Ecol. 44 (1), 219–225.

McVean, D.N., 1956. Ecology of *Alnus glutinosa* (L.) Gaertn. V. Notes on some British alder populations. J. Ecol. 44 (2), 321–330.

Miola, A., Bondesan, A., Corain, L., Favaretto, S., Mozzi, P., Piovan, S., Sostizzo, I., 2006. Wetlands in the Venetian Po Plain (North-Eastern Italy) during the Last Glacial Maximum: Vegetation, hydrology, sedimentary environments. Rev. Palaeobot. Palynol. 141 (1), 53–81.

Moen, A., 1999. National Atlas of Norway - Vegetation. Norwegian Mapping Authority, Honefoss.

Monegato, G., Ravazzi, C., Donegana, M., Pini, R., Calderoni, G., Wick, L., 2007. Evidence of a two-fold glacial advance during the Last Glacial Maximum in the Tagliamento end moraine system (SE Alps). Quat. Res. 68, 284–302.

Monegato, G., Pini, R., Ravazzi, C., Reimer, P., Wick, L., 2011. Correlation of Alpine glaciation and global glacioeustatic changes through integrated lake and alluvial stratigraphy in N-Italy. J. Quater. Sci. 26 (8), 791–804.

Monegato, G., Ravazzi, C., 2018. The Late Pleistocene multifold glaciation in the Alps: updates and open questions. Alpine Mediterranean Quaternary 31, 225–229.

Monegato, G., Ravazzi, C., Culiberg, M., Pini, R., Bavec, M., Calderoni, G., Ježˇ, J., Perego, R., 2015. Sedimentary evolution and persistence of open forests between the southeastern fringe of the Alps and the Northern Dinarides during the Last Glacial Maximum. Palaeogeogr. Palaeoclimatol. Palaeoecol. 436, 23–40.

Nelson G., Earle C.J., Spellenberg R., 2014. Betulaceae: Birch Family In (A.K. Hughes Ed.) Trees of Eastern North America. Princeton University Press.

Monegato, G., Scardia, G., Hajdas, I., Rizzini, F., Piccin, A., 2017. - The Alpine LGM in the boreal ice-sheets game. Sci Rep. 7, 2078. https://doi.org/10.1038/s41598-017-02148-7.

Nilsson, O., Hjelmquist, H., 1967. Studies on the nutlet structure of South Scandinavian species of *Carex*. Bot. Notiser 120, 461–485.

Oberdorfer, E., 1977. Süddeutsche Pflanzengesellschaften. Teil I. Fischer, Stuttgart.

Oksanen, J., Blanchet, F.G., Kindt, R., Legendre, P., Minchin, P.R., O'Hara, R.B., Simpson, G.L., Solymos, P., Stevens, M.H., Wagner, H., 2019. Vegan: Community ecology package. R package version 2.2-1 http://CRAN.R-project.org/package=vegan.

Perala, D.A., Alm, A.A., 1990. Reproductive ecology of birch: A review. For. Ecol. Manag. 32 (1), 1–38.

Pereira, H., 2017. Cork: Biology, Production and Uses. Elsevier, Amsterdam.

Pini, R., Ravazzi, C., Reimer, P., 2010. The vegetation and climate history of the last glacial cycle in a new pollen record from Lake Fimon (southern Alpine foreland, N-Italy). Quat. Sci. Rev. 29, 3115–3137.

Punt, W., Blackmore, S. (Eds.), 1976-2009. The Northwest European Pollen Flora. vols. I-IX. Elsevier Publishing Company.

Rasmussen, S.O., Bigler, M., Blockley, S.P., Blunier, T., Buchardt, S.L., Clausen, H.B., Cvijanovic, I., Dahl-Jensen, D., Johnsen, S.J., Fischer, H., et al., 2014. A stratigraphic framework for abrupt climatic changes during the Last Glacial period based on three synchronized Greenland ice-core records: Refining and extending the INTIMATE event stratigraphy. Quat. Sci. Rev. 106, 14–28.

Ravazzi, C., Deaddis, M., De Amicis, M., Marchetti, M., Vezzoli, G., Zanchi, A., 2012. The last 40 ka evolution of the Central Po Plain between the Adda and Serio Rivers. Geomorphol. Relief, Process. Environ. 2, 131–154.

Reille, M., 1992-1998. Pollen et spores d'Europe et d'Afrique du Nord. Laboratoire de Botanique historique et palynologie, Marseille.

Reimer, P.J., Bard, E., Bayliss, A., Beck, J.W., Blackwell, P.G., Bronk Ramsey, C., Buck, C.E., Cheng, H., Lawrence Edwards, R., Friedrich, M., Grootes, P.M., et al., 2013. IntCal13 and Marine13 radiocarbon age calibration curves 0–50,000 years cal BP. Radiocarbon 55 (4), 1869–1887.

Rodwell, J.S. (Ed.), 1995. British Plant Communities, Vol. 4. Aquatic Communities, Swamps and Tall-Herb Fens. Cambridge University Press, Cambridge, p. 283.

Rotunno, R., Houze, R.A.J., 2007. Lessons on orographic precipitation from the mesoscale alpine programme. Q. J. R. Meteorol. Soc. 133, 811–830.

Sanchez Goñi, M.F., Landais, A., Fletcher, W.J., Naughton, F., Desprat, S., Duprat, J., 2008. Contrasting impacts of Dansgaard– Oeschger events over a western European latitudinal transect modulated by orbital parameters. Quater. Sci. Rev. 27, 1136–1151.

Schneider, R., Tobolski, K., 1985. Lago di Ganna - Late Glacial and Holocene environments of a lake in the Southern Alps. Dissert. Bot. 87, 229–271.

Schulze, E.-D., Wirth, C., Mollicone, D., Ziegler, W., 2005. Succession after stand replacing disturbances by fire, wind throw, and insects in the dark Taiga of Central Siberia. Oecologia 146, 77–88.

Schweingruber, F.H., 1990. Anatomie europaischer Holzer. Ein Atlas zur Bestimmung europäischer Baum-, Strauch- und Zwergstrauchhölzer. Verlag Paul Haupt, Bern und Stuttgart, p. 800.

Schweingruber, F.H., Steiger, P., Börner, A., 2019. Bark Anatomy of Trees and Shrubs in the Temperate Northern Hemisphere. Springer, Berlin.

Seppälä, M., 1997. Distribution of permafrost in Finland. Bull. Geol. Soc. Finland 69 (1–2), 87–96.

Shaw, K., Stritch, L., Rivers, M., Roy, S., Wilson, B., Govaerts, R., 2014. Betulaceae. Botanical Gardens Conservation International, Richmond, UK.

Shibui, H., Sano, Y., 2018. Structure and formation of phellem of *Betula maximowicziana*. IAWA J. 39 (1), 18–36.

Spötl, C., Mangini, A., 2007. Speleothems and paleoglaciers. Earth Planet. Sci. Lett. 254, 323–331.

Spötl, C., Reimer, P.J., Starnberger, R., Reimer, R.W., 2013. A new radiocarbon chronology of Baumkirchen, stratotype for the onset of the Upper Würmian in the Alps. J. Quat. Sci. 28 (6), 552–558.

Svenning, J.C., Skov, F., 2004. Limited filling of the potential range in European tree species. Ecol. Lett. 7, 565–573.

Ter Braak, C.J.F., Prentice, I.C., 1988. A theory of Gradient Analysis. Advance in. Ecol. Res. 34, 235–282.

Teskey, R.O., Saveyn, A., Steppe, K., McGuire, M.A., 2008. Origin, fate and significance of CO_2 in tree stems. New Phytol. 177, 17–32.

Tutin, T.G., et al. (Eds.), 1968. Flora Europaea, First ed. Rosaceae to Umbelliferae Vol. II. Cambridge University Press, Cambridge.

Tutin, T.G., et al. (Eds.), 1980. Flora Europaea. Volume V. Alismataceae to Orchidaceae (Monocotyledones), First. ed. Cambridge University Press, Cambridge.

Tutin, T.G., et al. (Eds.), 1993. Flora Europaea. Volume I. Phsylotaceae to Platanaceae, Second ed. Cambridge University Press, Cambridge.

Tzedakis, P.C., Lawson, I.T., Frogley, M.R., Hewitt, G.M., Preece, R.C., 2002. Buffered tree population changes in a quaternary refugium: Evolutionary implications. Science 297, 2044–2047.

Tzedakis, P.C., Emerson, B.C., Hewitt, G.M., 2013. Cryptic or mystic? Glacial tree refugia in northern Europe. Trends Ecol. Evol. 28 (12), 696–704.

Dinter, M. van, Birks, H.H., 1996. Distinguishing fossil *Betula nana* and *B. pubescens* using their wingless fruits: Implications for the late-glacial vegetational history of western Norway. Veget. Hist. Archaeobot. 5, 229–240.

Vezzoli, G., Garzanti, E., 2009. Tracking paleodrainage in Pleistocene Foreland basins. J. Geol. 117, 445–454.

Waelbroeck, C., et al., 2019. Consistently dated Atlantic sediment cores over the last 40 thousand years. Sci. Data 6, 6–165.

Walter, H., 1968. Die Vegetation der Erde in öko-physiologischer Betrachtung. Bd. II. Die gemässigten und arktischen Zonen, Jena, Stuttgart.

Walter, H., Breckle, S.-W., 1986. Ecological systems of the geobiosphere. 3 Temperate and Polar Zonobiomes of Northern Eurasia. Springer, Berlin.

Whitlock, C., Larsen, C., 2001. Charcoal as a fire proxy. In: Smol, J.P., Birks, H.J.B., Last, W.M. (Eds.), Tracking Environmental Change Using Lake Sediments. Terrestrial, Algal, and Siliceous Indicators Volume 3. Kluwer Academic Publishers, pp. 75–97.

Wohlfarth, B., Veres, D., Ampel, L., Lacourse, T., Blaauw, M., Preusser, F., Andrieu-Ponel, V., Kéravis, D., Lallier-Vergès, E., Björck, S., Davies, S.M., de Beaulieu, J.-L., Risberg, J., Hormes, A., Kasper, H.U., Possnert, G., Reille, M., Thouveny, N., Zander, A., 2008. Rapid ecosystem response to abrupt climate changes during the last glacial period in western Europe, 40–16 ka. Geology 36 (5), 407–410.

Kalliola, R., 1973. Suomen Kasvimaantiede. Werner Söderström Osakeyhtiö, Helsinki (in Finnish).

R Core Team, 2013. R: A language and environment for statistical computing. R Foundation for Statistical Computing, Vienna, Austria. URL http://www.R-project.org/